

Alexander Mache, BSc

CALCIUM SULFOALUMINATE CEMENT FOR DRY-MIX SHOTCRETE ACCELERATION

Master thesis

Submitted in Partial Fulfilment of the Requirements for the Degree of

Master of Science

Geoscience – Engineering Geology

at Graz University of Technology (TU Graz)

Supervisors

Dr. Galan Garcia Isabel

Institute of Applied Geosciences

Dipl.-Ing. BSc Briendl Lukas

Dr. Mittermayr Florian

Institute of Technology and Testing of Construction Materials

STATUTORY DECLARATION

I declare that I have authored this thesis independently, that I have not used other than the declared sources / resources, and that I have explicitly marked all material which has been quoted either literally or by content from the used sources. The text document uploaded in TUGRAZonline is identical to the present master thesis.

Graz,

date

.....

(signature)

Acknowledgement

I thank all the people who made the completion of this master thesis possible.

I would like to pay my special regards to Dr. Isabel Galan for providing me valuable guidance as a supervisor throughout this thesis. Without her expertise in mineralogy and material sciences, the goal of this master thesis would not have been realized. But most importantly, her wholehearted character and willingness to answer all my questions never failed to support me.

My thanks to Dipl.-Ing. Lukas Briendl for sharing his technical knowledge with me and for always explaining and organizing the laboratory and real scale experiments.

I wish to show my gratitude to Florian Steindl MSc BSc for helping me in all software related issues.

A special thanks to my family. Words can not express how grateful I am to my parents, for their financial support and for always believing in me and my abilities. I want to thank my brother Lukas and my grandparents for always encouraging me throughout this experience.

Finally, I would like to thank my girlfriend Valentina, for her love and unconditional support.

I dedicate this master thesis to my brother Stephan †

Abstract

Shotcrete or sprayed concrete is typically used in underground construction and excavation processes, where heavy framework is difficult to install. Especially in confined spaces dry-mix shotcrete applications come in handy because of the small equipment. To achieve the challenging shotcrete requirements of fast setting and rapid strength gain, setting accelerators or special fast-setting binders are used. Due to the alarming effects caused by climate change, the concrete industry is under increasing pressure to reduce the energy used in the clinker production and related CO₂ emissions generated through the degassing of limestone. As a result, there is a gaining interest in the implementation and development of alternative binders to Portland cement (PC) in concrete and shotcrete. One of the most promising substitutes to PC is calcium sulfoaluminate (CSA) cement, with notably less CO₂ emissions during production. Recent studies have shown that the presence of CSA can increase the early strength development of shotcrete. The exact mechanisms and reactions, as well as the CSA-PC mixes optimization for shotcrete, have not been yet thoroughly assessed. In this work CSA cement was used to replace PC in dry mix shotcrete blends. Various PC/CSA ratios were analysed by visual tests, isothermal calorimetry, X-ray diffraction, scanning electron microscopy and compressive/flexural strength measurements in order to understand the impact of CSA mixed with PC and to create a suitable shotcrete mix for real scale spraying. In the laboratory tests, two mixes containing 1% CSA and 0.1% citric acid achieved an estimated setting time of 40-60 seconds, considered suitable for shotcrete applications. CSA worked like an accelerator in those two mixes, promoting the ettringite formation in the first minutes after hydrating the cement and giving the cement the necessary early age strength for shotcrete usage. The small amount of citric acid slowed down the reaction for about 20 seconds and worked like a retarder. Isothermal calorimetry results showed that mixes with more than 10% CSA content had no acceleration period after 4-6h and therefore no C-S-H formation, resulting in failing compressive strength tests. During the real scale spraying tests up to 30% higher early compressive strengths were achieved by those two mixes (1% CSA) during the first 24h compared to a reference mix prepared with a commonly used PC-based spray binder. The results obtained have shown that small amounts of PC can be replaced by CSA in order to achieve good early age strength exceeding J3 the highest strength class for shotcrete without using of conventional accelerators.

Abbreviations

AFm	A luminat e F errite m onosulfate
Bwb	B y w eight of b inder
C ₂ S	Dicalcium Silicate (Belite)
C ₃ A	Tricalcium aluminate
C ₃ S	Tricalcium silicate (Alite)
C ₃ FT	Tricalcium ferrotitanate
C ₄ AF	Tetracalcium aluminoferrite (Ferrite)
C ₄ A ₃ \$	Tetracalcium Trialuminium sulfate (Ye'elemite)
C ₆ AF ₂	Hexacalcium aluminoferrite
CA	C itric A cid
C-A-H	C alcium A luminat e H ydrates
CEMI	CEM I 52.5R acc. to EN 197-1
CSA	C alcium S ulfoaluminat e cement
CSA CK	CSA Alpenat CK
CSA R ²	CSA Alpenat R²
C-S-H	C alcium S ilicat e H ydrates
GGBS	G round g ranulat e d b last f urnace s lag
PC	P ortland c ement
SCMs	S upplementary c ementit i ous m aterials
SEM	S canning E lectron M icroscope
SRO	CEM I- SRO 52.5N
XRD	X - R ay D iffraction

Table of contents

Acknowledgement	I
Abstract	II
Abbreviations	III
1. Introduction	1
1.1. Shotcrete	1
Wet-mix shotcrete	2
Dry-mix shotcrete	3
1.1.1. Shotcrete components and mixes	4
Cements	4
Supplementary cementitious materials (SCMs) and fillers	4
Aggregates	5
Admixtures	5
Additional components	6
Shotcrete mixes	6
1.1.2. Hydration of shotcrete	7
1.2. Calcium Sulfo-Aluminate Cement (CSA)	8
1.3. CSA shotcrete	9
2. Experimental	11
2.1. Materials	11
2.1.1. Portland cements	11
2.1.2. Spray binder	11
2.1.3. Calcium sulfoaluminate (CSA) cements	13
2.1.4. Ground granulated blast furnace slag	14
2.1.5. Retarder admixture	14
2.1.6. Additional Ca(OH) ₂ , Gypsum and Anhydrite	14
2.1.7. Aggregates	15
2.2. Mixes	15
2.3. Laboratory tests	16
2.3.1. Visual tests	16
2.3.2. Isothermal Calorimetry	17
2.3.3. Compressive/flexural strength tests	18
2.3.4. X-Ray Diffraction	20
2.3.5. Scanning Electron Microscopy	22
2.4. Real scale tests	24
2.4.1. Needle Penetration test	25

2.4.2.	Stud driving method	26
2.4.3.	Drill cores and compressive strength	27
3.	Results	27
3.1.	Laboratory results	28
3.1.1.	Visual tests	28
3.1.2.	Isothermal calorimetric analyses	28
3.1.3.	XRD-measurements	34
3.1.4.	Compressive/flexural strength	40
3.1.5.	SEM results	42
3.2.	Real scale results	44
3.2.1.	Compressive early age strength development	45
3.2.2.	Compressive strength	45
4.	Discussion	47
5.	Conclusions	51
	References	52
	Appendix	55
	List of tables	57
	List of figures	58

1. Introduction

1.1. Shotcrete

Shotcrete, also known as sprayed concrete, is concrete projected at high velocity onto a surface (Fig. 1). Taxidermist Carl Akeley constructed the first machine to spray concrete in 1907: the dry material was blown out of a hose and the water was then injected at the nozzle. The device was used to repair the crumbling façade of the Field Columbian Museum in Chicago (Teichert, 2002). The



Figure 1: Shotcrete-stabilized cliff wall (Tikkanen et al., 2019)

sprayed/shot concrete sticks to the object, among others by its own pressure resulting from the “shooting process”. Therefore, the object must be clean, solid and rough. Usually the application of shotcrete requires a framework of reinforced bars and/or a steel mesh, but due to its very good adhesion properties and the versatility of the application method any shape is possible. At first sprayed concrete was used for reinforced concrete repair work. Nowadays typical uses and applications are underground constructions such as primary and secondary tunnel linings, shaft constructions and storage reservoirs. In addition to that, shotcrete is also used to build shell roofs, fire-protective layers and dams, to name just a few fields of application. Large volumes of sprayed concrete can be applied quickly and economically. Tunnel linings or retaining walls can be sprayed immediately after excavation (Fig. 2). The flexibility and ease of application enables the shotcrete to be applied in restricted and dangerous areas, where only the operator and the spraying equipment need to be onsite with no need of transport and set up of bulky formwork.

Late compressive strength (from 28 days onwards) of shotcrete does not differentiate much from that of ‘standard’ poured concrete. However, early age strength development is one of the most important characteristics of sprayed concrete which makes it different from concrete: compressive strength of shotcrete can reach 8 MPa in 5 hours and up to 20 MPa in 24 hours. (Sprayed Concrete Association, 2016) The other important property of shotcrete is the very fast setting, which is achieved by various methods, including the use of setting accelerators. As a result of the high velocity impact on the surface, sprayed concrete usually shows high density and low permeability. However, inhomogeneity and surface cracking due to shrinkage are common issues in shotcrete applications.



Figure 2: Primary tunnel linings (Sprayed Concrete Association, 2016)

In terms of the application method of shotcrete, there are two main procedures: the wet-mix and the dry-mix versions.

Wet-mix shotcrete

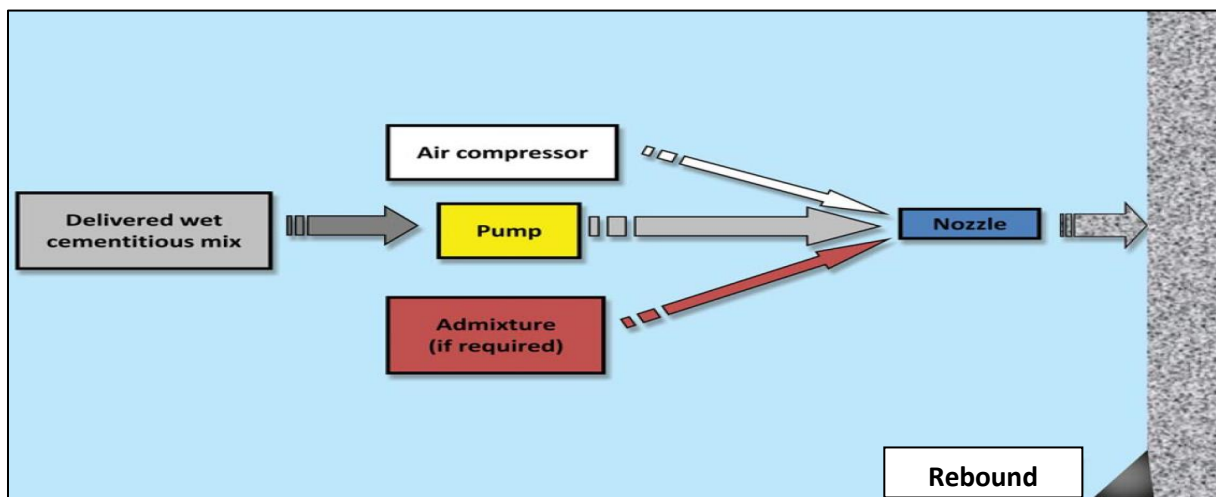


Figure 3: Simplified display of wet-mix-process (Sprayed Concrete Association, 2016)

The wet-mix method (Fig. 3) requires a previously made mixture of cement, aggregates and water, that is, a concrete, which is then pumped to the nozzle in a fluid state. At the nozzle compressed air is forced into the system to accelerate and “shoot” the finished mixture onto

the objective, where the concrete gets compacted by its own momentum. The balance of fine and coarse aggregates, usually between 0 and 8 mm, is an important parameter which determines the rebound and the maximum pumping rates, among others. With the use of the wet-mix process, concrete layers up to 300 mm are usually applied but the thickness varies with the nature of the task. Additional layers can be sprayed once the previous layer has reached a final set. Using plasticisers, also known as water reducers, water/cement ratios can be reduced up to 40% (Höfler et al., 2012). The fluid state of the wet mix concrete can be extended up to 72 hours by adding retarding admixtures to the system, which allows high flexibility for the application of the concrete. Additionally, setting accelerators are commonly injected at the nozzle to ensure fast setting and acceleration of the hydration process of the shotcrete. Wet-mix concrete requires cement contents between 350 and 450 kg per cubic meter. Usually cube compressive strengths between 30 and 60 N/mm² are reached after 28 days. Especially in underground construction and excavation sites, where heavy framework is difficult to install, wet shotcrete is used to secure and cover exposed rock surfaces and loose soils. Wet mix shotcrete can also be applied for the installation of permanent linings, temporary support or water flows channelling in tunnels. Its high-volume output, up to 25 m³/h, the relatively small equipment and the early strength development are some additional benefits, why wet shotcrete is used in underground excavation (Sprayed Concrete Association, 2016). In general, machines with piston and worm pumps are used to carry the concrete to the nozzle. The design of the machine (worm-pump, double-piston, rotor-chamber) determines the throughput and quality of the final product: ideally, the spraying equipment should deliver concrete in regular rates and be free from pulsation effects that can cause admixtures overdosing (Sprayed Concrete Association, 2016).

Dry-mix shotcrete

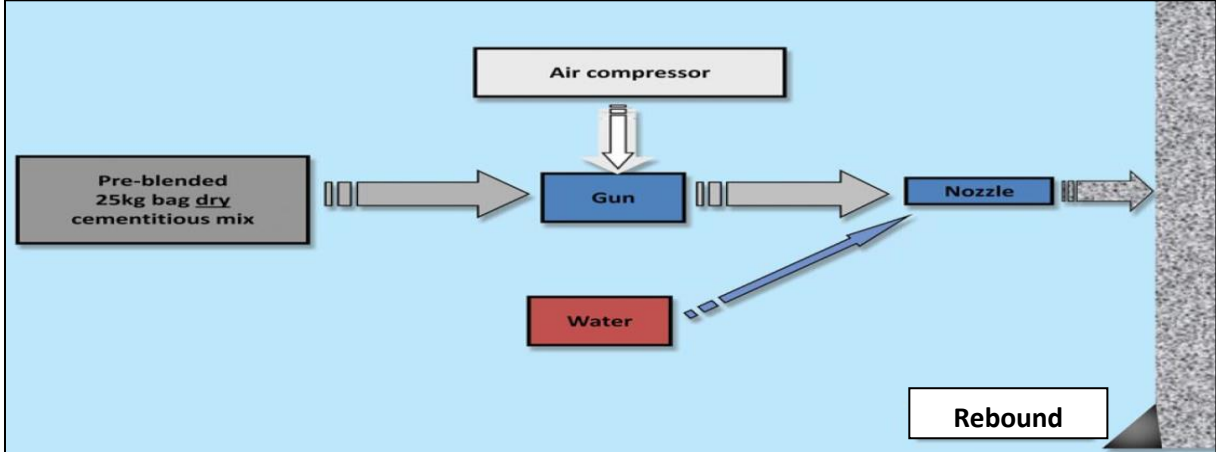


Figure 4: Simplified display of dry-mix-process (Sprayed Concrete Association, 2016)

In the dry process (Fig. 4), the solid components of the concrete, mainly cement and aggregates, are pre-mixed. A high velocity air stream carries the dry mix through a flexible hose to the nozzle, where the water is added to the dry mix. Materials can be projected with high velocity into place, where the impact compacts the concrete. Dry-mix sprayed concrete with adequate aggregate/cement ratios can be applied at relatively low water/cement ratios (0.4). Those features enable the material to be applied on vertical and overhead surfaces without slump characteristics (Sprayed Concrete Association, 2016). Usually the nozzle is operated handheld by one specialist, who adjusts the added amount of water. Aggregate/cement mass ratio normally varies between 2/1 and 4/1. The main disadvantages of the dry-mix process, compared with the wet-mix, are the higher dust emissions, higher rebound and lower volume output. The rebound of the sprayed mix contains a higher proportion of coarse aggregate, making the final result richer in cement than the original dry-mix. Typical areas of dry-mix shotcrete application are confined spaces where only small equipment can be used.

The most commonly used machines for dry-mix shotcrete these days are rotor-type machines, in which the aggregate-cement mixture is added to an open hopper that leads into a revolving barrel. The nozzle can be up to hundred meters away from the machine. Modern machines produce outputs up to 10 m³/h and can handle a moisture content in the dry mix of 10% (Sprayed Concrete Association, 2016).

1.1.1. Shotcrete components and mixes

Cements

Mostly Portland cements of the classes CEM I or CEM II are used for wet-mix spraying concrete applications. In the case of dry-mix applications, apart from standard CEM I cements, rapid hardening or fast-setting binders, so called spray-binders, can be used. In the Alps region, spray binders with very low sulfate content are mostly used (Galan et al., 2019).

Both types of cements contain mainly 4 clinker phases: alite (tricalcium silicate), belite (dicalcium silicate), aluminat (tricalcium aluminat) and ferrite (tetracalcium ferroaluminat). Apart from these clinker phases, the cements contain sulfate source phases like gypsum, anhydrite, bassanite or arcanite.

Supplementary cementitious materials (SCMs) and fillers

Today most shotcrete mixtures contain supplementary cementitious materials (SCMs) that add up to the binder in shotcrete. In general, those materials are by-products from other

industrial processes or natural materials. SCMs contribute to certain properties of the concrete by showing either pozzolanic, hydraulic or a physical behaviour, usually referred to as filler effect (Lothenbach et al., 2011).

A pozzolanic SCM is a siliceous or siliceous/aluminous material that has little or no cementitious value by itself, but which reacts, in the presence of moisture, with calcium hydroxide to form constituents having cementitious properties (Mehta et al., 1987). Typical pozzolana are fly ash, silica fume, volcanic glass, metakaolin and calcined shale or clay.

(Latent) hydraulic SCMs form cementitious phases in the presence of water through a hydration reaction. However, most of these binders show a relatively low hydraulic activity compared to Portland cement. In order to accelerate the hydration reaction sulfates, alkali-hydroxides, lime or lime producing materials like Portland cement are added to the cementitious mix. Hydraulic SCMs can replace Portland cement to a much larger extent than pozzolana. One of the most commonly used hydraulic SCM in shotcrete applications is ground granulated blast furnace slag (GGBFS). This material is obtained from the pig iron production process by-product called molten iron slag, rapidly cooled down to $\sim 800^{\circ}\text{C}$, dried and ground. GGBFS alone has no hydraulic properties and does not harden when mixed with water. However, during hydration with OPC (or $\text{Ca}(\text{OH})_2$), GGBFS gets activated and forms calcium silicate hydrates (C-S-H), similar to those forming from Portland cement hydration, but with lower calcium/silicon ratios (Stark et al., 2000).

Aggregates

The selection of aggregates includes petrographic, grain shape and grain size distribution criteria. To ensure a steady flow through the system (pumping device, hose, nozzle), typically aggregate sizes between 0-8 mm are used. Specifically, in Austria the aggregates used have to comply with ÖNORM B 3131 and ÖNORM EN 12620.

Admixtures

In many applications sprayed concrete requires the use of admixtures to improve certain properties of the fresh mix and the hardened concrete. Frequently used admixtures are:

- Setting accelerators: There are various types of setting accelerators for shotcrete. The most commonly used liquid accelerators for wet-mix shotcrete in the Alps region are based on aluminium-(hydroxi)-sulfate, and free from alkali. Other commonly used accelerators in other parts of the world include those based on sodium silicate, however its use implies health risks and, although the accelerators have a positive effect in the setting and early strength development, they can negatively impact the

final strength and thus the durability of the shotcrete (Millette et al., 2014). Accelerator dosage depends on the mix and type of accelerator. For aluminium sulfate-based accelerators in tunnel applications around 6-12% accelerator (referred to the binder mass) is used (Austrian Building Technology Association, 2013). In the case of dry-mix shotcrete, powder accelerators are sometimes used when no special fast-setting binders are used and high early strength is required. Most common chemical compositions include (sodium and calcium) aluminates and carbonates, and the dosage varies generally between 2 and 8% (Myrdal et al., 2007).

- **Superplasticisers:** The use of superplasticisers allows to reduce the water in the fresh shotcrete maintaining high workability with no, or just a little, retardation of the mix. The molecules of the plasticisers separate the particles of the cement with steric/electrostatic forces, resulting in beneficial effects for various processes, including pumping, transport, spraying and compaction (Nkinamubanzi et al., 2016).
- **Retarders:** Ideally, without reducing the quality of the final sprayed concrete, these admixtures maintain workability of sprayed concrete during transportation and application. Commonly used retarders include sugars, hydroxycarboxylic acids and phosphates. Various mechanisms are responsible for the retardation in the cement-water system, including precipitation, complexation, adsorption and nucleation (Myrdal et al., 2007).

Additional components

Reinforcing fibres (steel or polypropylene) are sometimes included in the shotcrete mix to reduce the propagation of shrinkage cracks and improve the structural strength, among others. The suitability of its use depends mostly on the type of rock and the loads necessities; however, cultural, historical and economic factors play also a big role. For example, the use of steel fibres in the Scandinavian countries, with mainly granite rock, is generalised, whereas in the Alps region, fibres are used in very few cases. (Cengiz et al., 2004).

Shotcrete mixes

Typical compositions for 1 m³ of wet- and dry-mix shotcrete are shown in the following table.

Table 1: Typical mixing ratios of wet-mix and dry-mix shotcretes.

	binder	aggregates (0-8 mm)	water	super plasticisers (PCE)(bwb)	accelerator (bwb)
	[kg]	[kg]	[L]	[%]	[%]
wet-mix	400	1900	200	1	8
dry-mix	360	1900	180	-	-

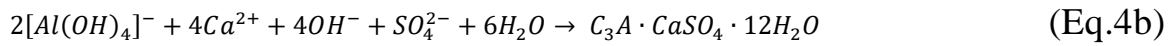
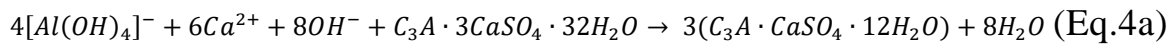
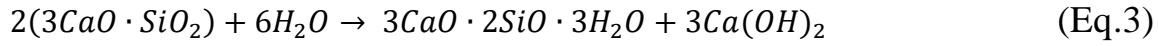
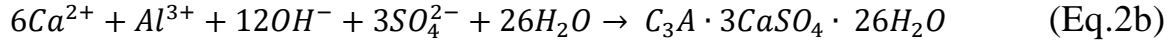
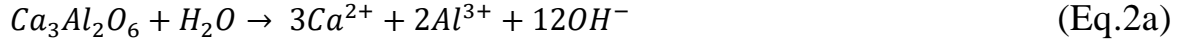
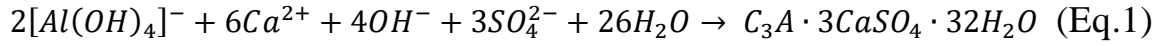
1.1.2. Hydration of shotcrete

The hydration processes in concrete and shotcrete are responsible for the development of the mechanical properties. Basically, the same hydration products (ettringite, AFm, portlandite, C-S-H) form in both cases; however, the formation rate and the relative amount of each phase formed can vary considerably in shotcrete and concrete. In the case of wet-mix shotcrete accelerated by means of aluminium sulfate-based accelerators, immediately after the accelerator is mixed with the concrete, massive amounts of ettringite are formed (Salvador et al., 2016; Paglia et al., 2001). The formation of this phase is mainly the result of the reaction of the $Al_2(SO_4)_3$ from the accelerator with the calcium dissolved from the cement phases (Eq. 1), and to a lower extent to the reaction of the dissolved C_3A (Eq. 2a) with the available sulfate dissolved at that point (Eq. 2b) (Pourchet et al., 2009). Ettringite is responsible for the fast setting and for the early development of strength. During the next few hours, the so-called induction period, hydration reactions progresses quite slow up to a point where the silicate reaction starts to be very significant. The reaction of C_3S with water leads to the formation of C-S-H and portlandite (Eq. 3), C-S-H being the main strength-giving phase in the system.

In these systems, the acidic nature of the aluminium sulfate based accelerator and the early consumption of calcium ions used to form ettringite favour the earlier dissolution of alite, which in turn promotes earlier formation of silicate hydrates. If the ratio Al/S in the accelerator is lower than that in ettringite, sulfate from the cement system may be needed to form ettringite from the available calcium and aluminium, leading to an earlier sulfate depletion and earlier formation of AFm phases (Eq. 4a and 4b) (Salvador et al., 2016).

In the case of spray binders hydration reactions differ, especially at early stages. Due to the low sulfate content in the clinker, the rapid hydration of the tricalcium aluminate phase (C_3A) and the formation of C-A-H phases are mostly responsible for the fast setting and the early strength development. Further on, similarly to wet-mix concrete, alite hydration leads

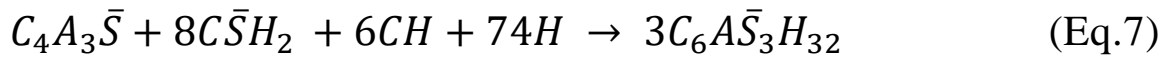
to formation of portlandite and C-S-H, responsible for the further development of strength (Galan et al., 2019).



1.2. Calcium Sulfo-Aluminate Cement (CSA)

Calcium sulfoaluminate (CSA) cements contain ye'elemite ($C_4A_3\bar{S}$), as a main component, and belite (C_2S) in various ratios. Additionally, they contain calcium sulfate (mostly gypsum, but sometimes also anhydrite) and other phases such as ferrite, gehlenite and calcium aluminate. Ye'elemite was first introduced in the 1960s and patented by Alexander Klein as a shrinkage compensating addition to cementitious binders (Klein, 1963). Since then, CSA cements have been mainly implemented in China for the construction of concrete pipes, bridges and waterproof layers, and also in leakages, low temperature construction and shotcrete. Recently, CSA cements are receiving increasing attention worldwide because of the lower CO₂ emissions during production compared with Portland cement: production of CSA cement can lead to ~60% reduction in emitted carbon dioxide (Sharp et al., 1999). Alite, which is the main clinker phase from Portland cement, releases 0.578 g CO₂ per g of cement, whereas calcium sulfoaluminate clinker releases only 0.216 g CO₂ per g of cement (Sharp et al., 1999). Another energy saving feature of CSA clinker is its firing temperature, 1250°C, about 200°C lower than that used for Portland cement clinker. In addition, CSA clinker is easier to grind than Portland cement clinker (Glasser et al., 2001). The fact that secondary and industrial waste products are easily implemented in the production process benefit CSA cements perception further (Ambroise et al., 2008; Zhang et al., 1999). The main drawback of CSA cements is the higher need of aluminium in the raw materials, which increases production costs. To overcome this disadvantage, scientists and industry are looking into ways of replacing bauxite by industrial by products such as fly ash, baghouse dust, scrubber sludge or phosphogypsum (Juenger et al., 2011).

One of the main characteristics of CSA is its ability to produce fast setting and high early strength concrete. These properties are controlled by the composition of the clinker and the sulfate phases. For example, different calcium sulfate contents are used to formulate self-stressing and expansive cements. Because of these special characteristics, CSA cements are also being used to improve the properties of certain Portland cement mixes (Weifeng et al., 2018). The hydration reactions of CSA cements are highly dependent on the sulfate availability. In the absence of calcium sulfate, ye'elimite reacts with water forming monosulfoaluminate and aluminium hydroxide according to Eq. (5), the kinetics of this reaction being fairly slow. During the hydration process of ye'elimite in the presence of calcium sulfate, ettringite, which is responsible for the early strength development, is formed according to Eq. (6). Once the calcium sulfate source is depleted, monosulfate starts to form, implying that the ratio between calcium sulfate and ye'elimite determines the ratio between monosulfate and ettringite. In the presence of calcium hydroxide, water and calcium sulfate, ye'elimite forms ettringite rapidly (Eq. 7) (Juenger et al., 2011). At later stages of hydration (various days/weeks), belite starts to react with AH_3 forming strätlingite (C_2ASH_8) (Eq. 8). In the absence of AH_3 belite forms C-S-H and portlandite (Wang 2010; Morin et al., 2011).



Proper formulations and thus optimal distribution of hydrates in CSA matrices (space-filling ettringite needles combined with the rest of the hydrates formed) produce low porosity and very dense microstructures (Juenger et al., 2011).

1.3. CSA shotcrete

As mentioned in the first section, shotcrete is mostly used to provide rock support in underground constructions. For this, fast setting and early strength development are required. CSA cements, with the additional potential advantage of reducing the shrinkage, one of the main drawbacks of Portland cement shotcrete, comply with these requirements. Additionally, the good bonding and strength of CSA shotcrete should allow for the

application of relatively thin layers (Bescher et al., 2013). Recent studies have shown that PC-CSA mixes used for shotcrete provide enhanced compressive strengths compared to reference PC-mixes and shrinkage reduction as a result of the expansive formation of ettringite in CSA systems (Ballou et al., 2013). Yu et al. observed that using CSA-CS-PC cement mixes led to an expansive behaviour and to an increase in strength up to the 28th day (Yu et al., 2017). The experiments of Reny et al. revealed the capabilities of CSA shotcrete applied pneumatically with commercial dry-mix shotcrete equipment (Reny et al., 2013). Testing the CSA-mix in different seasons (winter and summer) showed that the temperature of the mix had an effect on the early-age compressive strength. CSA shotcretes sprayed with 5°C material temperature reached the minimum of 7 MPa 3 hours later than the same mix with an ambient temperature of 27 °C. However, later-age compressive strengths were not impacted by temperature as all tests reached the targeted compressive strengths after 24h (10 MPa), 3 days (20 MPa), 7 days (30 MPa) and 28 days (40 MPa).

According to Bescher et al., strength up to 20 MPa at 90 minutes, 30 MPa at 3 hours and over 50 MPa at 24 hours can be reached with the use of CSA cement (Bescher et al., 2013). Furthermore, the authors highlight other advantages of the use of CSA cement for underground construction fast set time, high chemical stability, sulfate resistance and low porosity (Bescher et al., 2013).

The investigations from Paglia et al proved the accelerating properties of small amounts of CSA in combination with aluminium sulfate (AS) (6% in total) in mixes with OPC: small ettringite prisms formed, resulting in more coalescence points and connecting the cement grains (Paglia et al., 2001 and Paglia, 2000). Therefore, the setting time was shortened strongly compared to an OPC reference mix, from 6-7 hours to 15-40 minutes. The CSA-AS accelerator promoted as well the early hydration of C₃A and C₃S.

The Center for Applied Energy Research from the University of Kentucky, together with the company Minova USA Inc, and the University of Dundee, developed a new shotcrete mix based on CSA cements called Tekcrete Fast ® (Tadolini et al., 2017; Oberlink et al., 2016). The aim of their investigation was to create a rapid strength, high bonding shotcrete system for infrastructure repair and stabilization. According to the authors, Tekcrete Fast ® reaches 17.2 MPa at 15 minutes, 31 MPa at 1 hour and up to 55.2 MPa at 24 hours.

According to Ballou et al. CSA shotcrete can reach up to 25 MPa in an hour without any accelerator, resulting in a more efficient working cycle at construction sites, which is a big economic advantage. In addition, the authors report that the cooling of the CSA shotcrete

using water is not as critical as with PC-shotcretes. Furthermore, without accelerators, there is no need to worry about the right dosage linked with the possible cracking of the cement (Ballou et al., 2013).

Despite these promising results, the potential use of CSA for shotcrete is still at the early stages of research and development. The exact hydration mechanisms, the microstructure development, optimal formulations, durability properties, etc, are still big unknowns.

The aim of this research work was to develop optimal mixes containing CSA for dry-mix shotcrete, evaluating the influence of the composition on the hydrated phases development, and the mechanical strength, both in lab- and real-scale tests.

2. Experimental

2.1. Materials

In this chapter the main characteristics of the materials used in the laboratory and field experiments are described. The mineralogical composition of the Portland cements was determined through quantitative XRD (QXRD) measurements and the chemical composition was determined through X-ray fluorescence spectroscopy (XRF). The mineralogical composition of the CSA cements was obtained from the producer Vicat.

2.1.1. Portland cements

Two different Portland cements were chosen for the experiments: CEM I 52.5R and CEM I 52.5N SR0. Both cements are normed after ÖNorm EN 197-1 (2011). The main component of both cements is Portland cement ($\geq 95\%$), with a maximum of 5 % of minor constituents. The mineralogical and chemical composition of CEM I 52.5R, from now on CEM I, and CEM I 52.5N SR0, from now on SR0, is shown in tables 2 and 3. The main difference between both cements is the tricalciumaluminate (C_3A) content: 11.5 and 1.7% in CEM I and SR0, respectively.

2.1.2. Spray binder

Spray binder is a typical binder used in dry-mix shotcrete operations. As such, it was used for the reference mix in the field tests. The mineralogical composition of the spray binder used and the oxide composition are shown in tables 2 and 3, respectively.

Table 2: Mineralogical composition of CEM I, SR0 and spray binder (- = below detection limit)

Phase	CEM I	SR0	Spray-binder
	Weight (%)	Weight (%)	Weight (%)
Alite (C₃S)	55.0	58.2	59.1
Belite (C₂S β)	13.1	12.6	13.8
Aluminate ortho (C₃A)	10.8	1.2	3.7
Aluminate cubic (C₃A)	0.7	0.5	7.6
Ferrite	7.4	12.3	8.2
Periclase	4.2	-	1.0
Anhydrite	3.8	3.4	-
Arcanite	2.0	0.4	0.6
Bassanite	1.7	0.5	1.2
Calcite	0.9	9.5	0.5
Portlandite	0.3	0.9	2.5
Aphthitalite	-	0.5	0.7
Dolomite	-	-	0.8
wRp	5.4	4.6	5.2

Table 3: Chemical composition of CEM I, SR0, spray-binder and GGBS (- = below detection limit)

Oxide (wt.%)	CEM I	CEM SR0	Spray-binder	GGBFS
Na₂O	0.5	0.4	0.7	0.4
MgO	4.0	1.2	2.0	8.7
Al₂O₃	5.4	2.9	6.1	11.9
SiO₂	20.0	20.2	20.6	39.5
P₂O₅	0.1	0.1	0.3	-
SO₃	3.0	2.3	1.2	1.7
K₂O	1.0	0.4	0.7	1.0
CaO	61.5	64.0	63.4	34.6
TiO₂	0.2	0.2	0.3	0.5
MnO	0.1	0.1	0.1	1.4
Fe₂O₃	2.8	4.3	2.8	0.4
LOI	1.3	4.0	1.8	-

2.1.3. Calcium sulfoaluminate (CSA) cements

Two CSA cements were used for the investigations: Alpenat R² and Alpenat CK. Both CSA cements were manufactured in Saint Egrève (France) by the company Vicat. The mineralogical and chemical compositions are shown in tables 4 & 5. The main difference between these two CSA cements is the added anhydrite content: 18% in the Alpenat R² cement and 0% in the Alpenat CK. The clinker contains in both cases 0.4% anhydrite.

Table 4: Mineralogical composition of Alpenat CK and Alpenat R² (- = below detection limit)

Phase	Alpenat CK	Alpenat R²
	Weight (%)	Weight (%)
Ye'elemite (C₄A₃S)	54.3	41.8
Belite (C₂S β)	20.8	16.0
Belite (C₂S α'high)	8.3	6.4
Merwinite (C₃MS)	4.5	3.5
Anhydrite (C\$)	0.4	0.3
Free lime	0.2	0.2
Fe₂O₃	1.0	0.8
C₃FT	9.3	7.2
C₆AF₂	1.2	0.9
Added components:		
Anhydrite (C\$)	-	18.0
Limestone filler	-	5.0

Table 5: Chemical composition of Alpenat CK and Alpenat R²

Oxide (wt.%)	Alpenat CK	Alpenat R²
SiO₂	10.6	9.3
Al₂O₃	24.5	20.9
CaO	44.7	47.3
MgO	0.8	1.3
Fe₂O₃	9.7	8.5
TiO₂	1.3	1.2
K₂O	0.1	0.1
Na₂O	0.2	0.2

P₂O₅	0.1	0.1
Mn₂O₃	0.0	0.1
SO₃	4.3	10.0
SrO	0.1	0.1
Cl	0.0	0.1
LOI	3.8	1.2

2.1.4. Ground granulated blast furnace slag

The GGBS used throughout this research had a very similar particle size distribution as the used Portland cements (see table 6). The chemical composition of the GGBS is shown in table 3.

Table 6: Density and particle size characteristics of the powdery materials used

Sample Name	Material	ρ (density) [g/cm³]	BET [m²/g]	Blaine [cm²/g]	d₅₀ [μm]
CEM I	CEM I 52,5R	3.60	1.32	5300	7.1
SR0	CEM I 52,5N C ₃ A free	3.26	0.96	4193	8.0
CK	CSA Alpenat CK	3.01	n.a.	4650	10.8
R2	CSA Alpenat R ²	2.97	n.a.	4500	n.a
GGBFS	Blast furnace slag	2.91	0.91	3919	8.6

***n.a. not analysed**

2.1.5. Retarder admixture

Citric acid was used as a retarder admixture for the investigations. Many commercial retarders contain citric acid as one of their main constituents, yet exact chemical formulas of these commercial retarders are not accessible. In order to understand the influence on the hydration process better, ordinary citric acid (anhydrous citric acid, Carl Roth, purity > 99.5%) was used in the experiments.

2.1.6. Additional Ca(OH)₂, Gypsum and Anhydrite

In order to compensate for the lower dissolved calcium at earlier stages of hydration, because of the low C₃A content in the SR0 cement, Ca(OH)₂ was used to provide an extra calcium source in one of the mixes. Gypsum and anhydrite were used to implement more sulfate and calcium into the system.

2.1.7. Aggregates

Two different types of aggregate were used for the experiments. In the laboratory a quartz rich sand from Bad Fischau with a grain fraction between 0 and 4 mm was used. The field tests were performed with a coarser dolomite sand from Eberstein with a grain fraction between 0 and 8 mm. The grain size distribution of both sands is shown in figure 5.

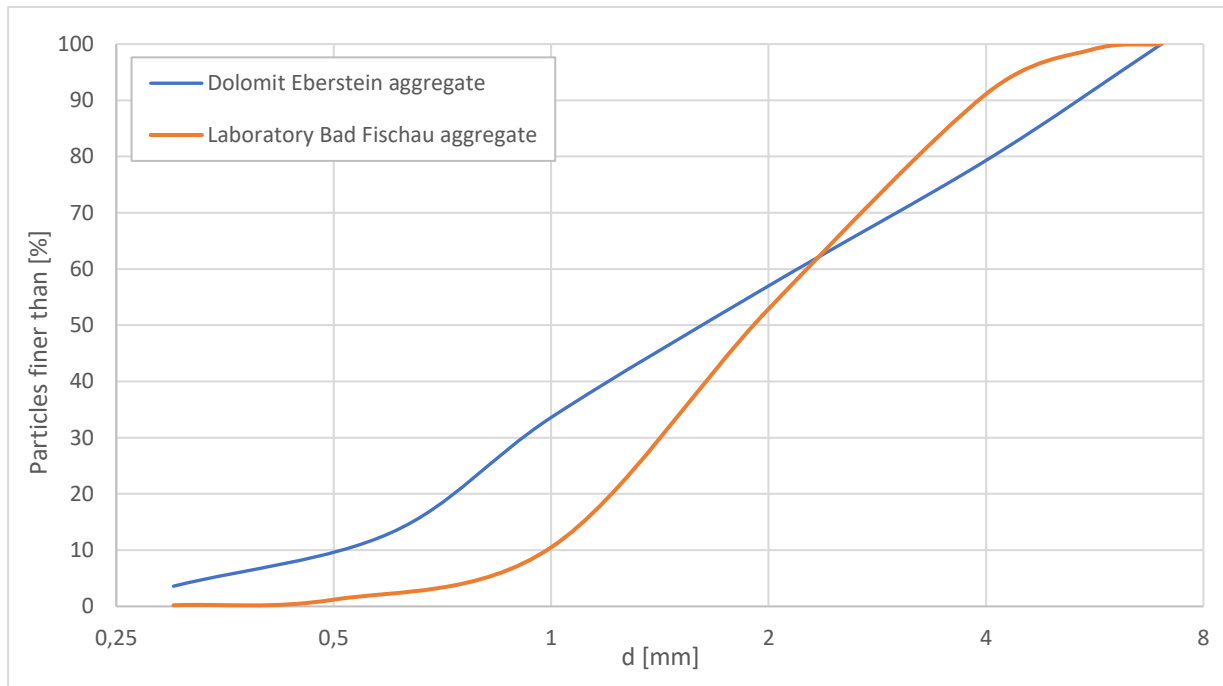


Figure 5: Grain size distribution of dolomite Eberstein and sand Bad Fischau according to ÖNORM B 3131

2.2. Mixes

Table 7 shows the compositions of the 22 mixes tested in the laboratory.

Table 7: Binder composition of the 22 tested mixes.

Sample	CEM I	SR0	CSA-CK	CSA-R ²	GGBS	Added components	Citric Acid	Gypsum	Anhydrite	Ca(OH) ₂	
Unit	%	%	%	%	%		%	%	%	%	
Mix 1	100										
Mix 2			100								
Mix 3	99		1				0.1				
Mix 4	79.2		0.8		20		0.1				
Mix 5	99		1								
Mix 6	60		40								
Mix 7	70		30								
Mix 8	80		20								
Mix 9	90		10				0.5				
Mix 10		50	50								
Mix 11		90	10								
Mix 12		90		10							
Mix 13		99	1							0.5	
Mix 14		100									
Mix 15	95		5								
Mix 16	10		90								
Mix 17			80					20			
Mix 18	67		25						8		
Mix 19		10	90								
Mix 20	90		5	5							
Mix 21	97		3								
Mix 22	98		2								

Table 8 shows the 3 mixes sprayed in the real scale spraying tests in Wopfing.

Table 8: Composition of the 3 different mixes tested and sprayed in Wopfing.

Name	P-1 (Ref)	P-11a	P-14
	%	%	%
CEM I		99.0	79.2
SPBM-2	80.0		
CK		1.0	0.8
GGBS	20.0	0.0	20.0
Water/cement	0.5	0.4	0.4
Added components			
Citric acid		0.1	0.1

2.3. Laboratory tests

2.3.1. Visual tests

22 cement pastes (without aggregates) were tested in the laboratory ‘visually’ (table 9). For this the samples were mixed with water manually, water/binder ratio 0.5, for 1 minute, with the help of a small spoon. The mixes were visually analysed in order to check whether the samples met the shotcrete requirement of fast setting in about 2 minutes.

2.3.2. Isothermal Calorimetry

Isothermal calorimetry measures the heat discharged or consumed by a chemical reaction. The calorimeter device keeps the temperature around the sample constant, with precision sensors measuring the heat generated by the reaction. The contact between the sample and the sample holder results in a heat generation (exothermic) or absorption (endothermic). The power consumed to keep the temperature of the

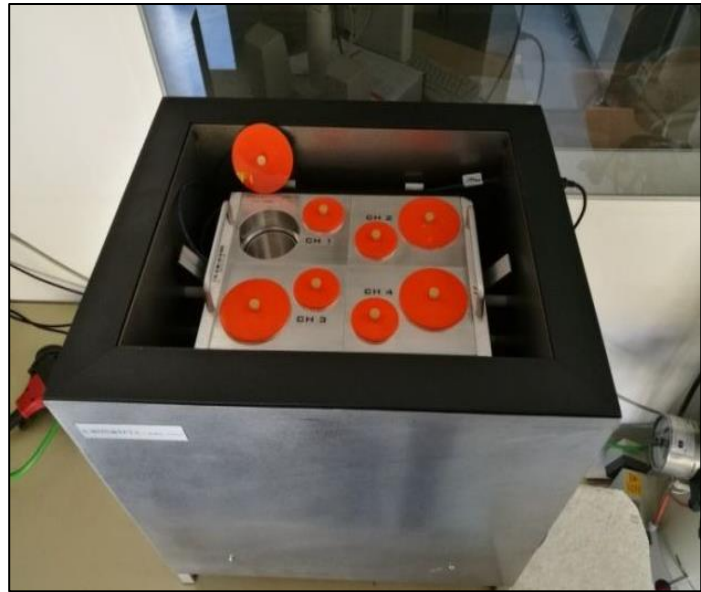


Figure 6: I-CAL 4000 HPC at TU Graz Inffeldgasse

samples surrounding constant is calculated by integrating the power over time, which displays the heat flow of the reaction. (Srivastava et al., 2019). Test temperatures from 5 up to 70°C can be used. Experiments are made at basically isothermal conditions because the heat produced in the sample is conducted away through heat flow sensors into a heat sink.

The heat generated by the hydration of a cementitious binder is an indicator for its rate of reaction because hydration reactions are exothermic. Fig. 7 shows the heat flow curve of mix 1 reference paste, with 100% cement in the binder, during the first 24 h of hydration. In the first minutes after adding water (stage I – pre induction period) anhydrite and clinker sulfates dissolve producing a sulfate-rich, alkaline solution. The most reactive clinker phase C_3A reacts with water and dissolves into an aluminium gel. With sulfate already present in the solution, ettringite is formed. This reaction is highly exothermic but does not last very long. Stage I is followed by a low heat period which lasts for about 3-4 hours (stage II – dormant or induction period). After 4 hours alite (C_3S) starts to form C-S-H and portlandite (stage III – acceleration/deceleration period).

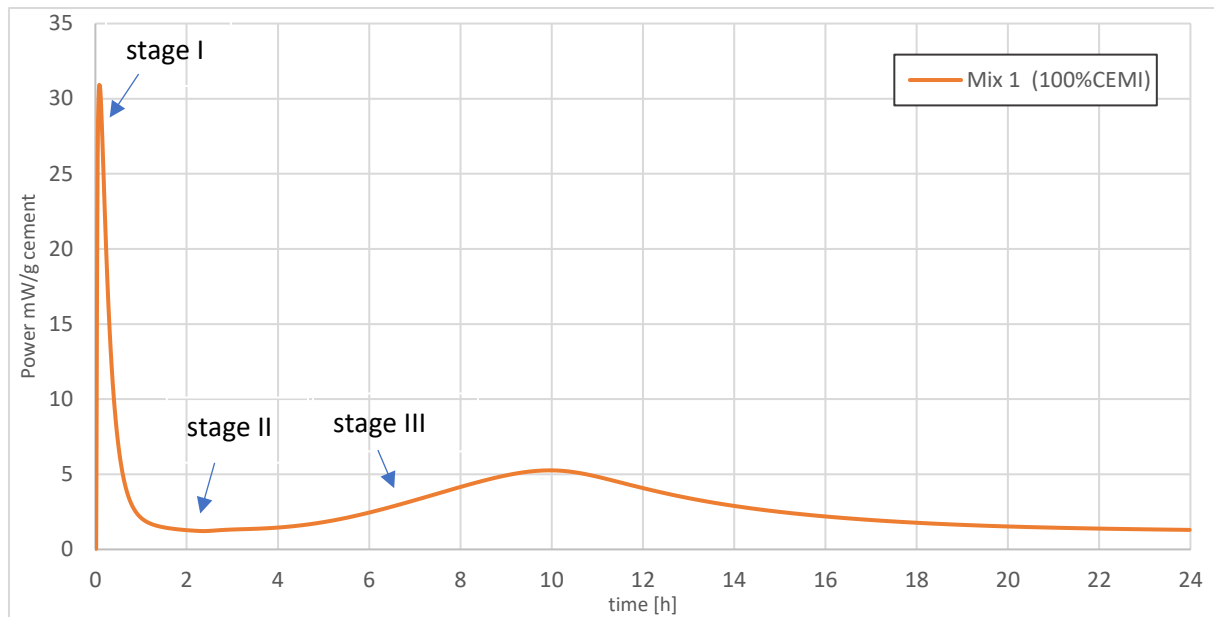


Figure 7: Heat flow curve of reference Mix 1

The calorimeter used for the experiments is located in the cement laboratory at the campus of TU Graz Inffeldgasse (Fig. 6). The I-CAL 4000 HPC (High Precision Calorimeter) is a 4 channel Calorimeter manufactured by the company “calmetrix”. The calmetrix software interface controls the ambient temperature around the sample and measures the heat flow of the cement hydration using precision sensors.

~50 grams of paste samples were prepared for the calorimetry measurements: binder and water, w/b 0.5, were manually mixed, for 1 minute, with the help of a small spoon. The samples were then transferred to the calorimeter to start the measurement (~2 minutes after first contact with water). The set temperature of the calorimeter was 20°C and its detection limit is at 1.1W. Measurements were taken every minute for 24h. Except for mixes 3, 6, 7 and 8, which were analysed every 10 seconds for the first 2 hours.

2.3.3. Compressive/flexural strength tests

The compressive strength test measures the maximum compression load a material can take before breaking or fracturing. Usually the tested samples are prisms, cubes or cylinders, which are placed between the two platens of the loading frame. The force gradually increases by moving one of the platens towards the other through hydraulic pressure. After the machine detects the breaking/fracturing of the sample, the maximum load is shown on the display in N. The compressive strength can be determined by dividing the failure load through the cross-sectional area of the sample resisting the load.



Figure 8: ToniPRAX compressive strength testing machine at TU Graz Inffeldgasse

The flexural strength test evaluates the concrete ability to withstand failure in bending by focusing the gradually increasing load on one point of the sample. The results represent the modulus of rupture, in MPa or N/mm². Mixture design, size and aggregate volume particularly influence the modulus of rupture, which is about 10 to 15 % of the concrete's compressive strength in general. For this research, a center point load test was used.

The compressive strength and the flexural strength of the mortar prisms were measured with a “ToniTechnik” Compression and Bending Test Plant “ToniPRAX”, located at the cement laboratory at TU Graz Inffeldgasse (see Figures 8 and 9). It is a combined testing machine for the standard-compliant testing of compressive (maximum load 300 kN) and flexural (maximum load 50 kN) strength of cement and other binding materials. According to EN 196 / ISO 679 the mortar prisms tested must be 40 x 40 x 160 mm.



Figure 9: ToniPRAX flexural strength testing machine at TU Graz Inffeldgasse

From the mixes that met the fast setting requirements, according to the visual observations, 3 mortar prisms were prepared to test the compressive and flexural strength after 6 h, 24 h, and 28 days. For the mortar 1200 g of aggregate, 600 g of cement and 300 g of water were mixed in a Hobart mixer. In some cases, citric acid was also added (see Table 7). To ensure a homogeneous mixing, the water was put in the mixer first, the cement/aggregate mix was added rapidly while the mixer was already working. After 20 seconds of mixing the mix was poured in a prism-steel case, which was then placed on a vibrating table (Fig. 10) for another 30 seconds in order to remove the air in the wet concrete and to distribute the mix evenly. Next, the prisms were



Figure 10: Prism-steel-case placed on the shaker before the mortar was poured in.

left to cure in a 99% relative humidity environment. After 6 hours the steel case was removed and the first flexural/compressive strength tests were performed. The two remaining prisms were placed under water until the last two tests (24h and 28 days) were performed.

2.3.4. X-Ray Diffraction

X-Ray diffraction is a technique used to identify the crystalline phases present in a sample. The principle of the method is based on the regular arrangement of atoms in crystal structures. The atoms electrons scatter the X-ray waves, emitted from the X-ray tube in a process called elastic scattering. Most emerging waves cancel each other out due to destructive interference, but in a few directions the waves add constructively, as described by Bragg's law (see Fig. 11).

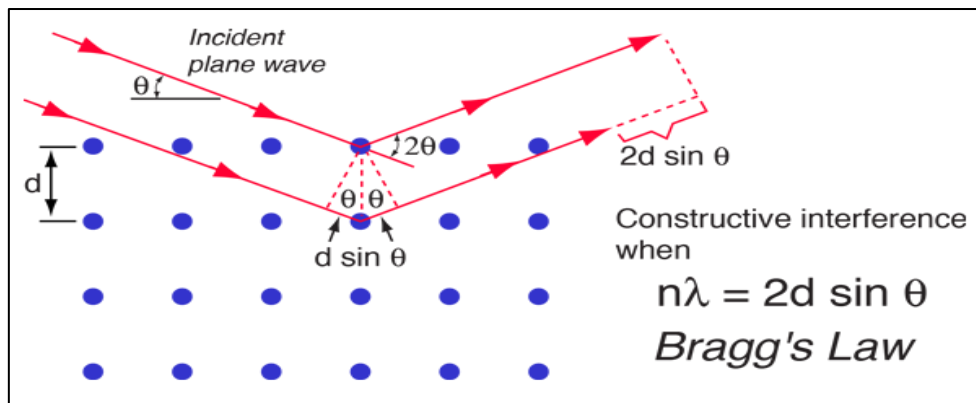


Figure 11: Bragg's Law (Thornton et al., 1993)



Figure 12: Sample changer and measurement device inside the Panalytical X'Pert Pro

The law states that when the x-ray is incident onto a crystal surface with a certain angle of incidence (θ), it will be reflected with the same angle of scattering (θ). And, when the path difference (d) is equal to a multiple of the wavelength, a constructive interference will occur. The scattered waves resulting from the constructive interference can be collected through a detector. Knowing the wavelength of the X-rays, the lattice plane distance (d) can be calculated and the unit cell of the analysed crystal system can be identified.

The institute of applied geoscience at the TU Graz Rechbauerstraße features an X-Ray diffractometer (Panalytical X'Pert Pro X-Ray Diffraction, Fig. 12 and 13) with a cobalt anode (40kV, 40mA) that is used throughout all experiments to provide mineralogical analysis of the samples.



Figure 13: X-Ray diffractometer Panalytical X'Pert Pro at TU Graz Rechbauerstraße

The software “Highscore Plus” and the ICSD (Inorganic Crystal Structure Database) is used for the identification of the crystalline phases. In-situ XRD measurements were carried out for 24 hours in samples covered with a Kapton film (Fig. 14) to prevent contact with the atmosphere. Scans were collected every 15 minutes from 9° to $50^\circ 2\theta$ and with a step size of 0.017.



Figure 14: Kapton film on a sample used for a 24h In-situ measurement

Single XRD scans were performed in some selected samples (mix 3 and 4) after 14 days of hydration. Scans were collected from 7° to $80^\circ 2\theta$ and with a step size of 0.017.

2.3.5. Scanning Electron Microscopy

The scanning electron microscope (Fig. 15) produces images of the sample by scanning the surface with a focused beam of electrons in a raster pattern. The SEM uses high vacuum to observe the specimens. To produce an image the electron beam interacts with the atoms at various depths of the sample. Secondary electrons (SE) and back scattered electrons (BSE) are reflected by the sample and get collected by detectors. Scintillators and photomultipliers amplify those signals, which are then displayed on a monitor.

The samples need some preparation to stabilize them and to increase their electric conductivity. Non-conducting material is coated with an ultrathin layer of conducting material, like gold/palladium, gold or graphite, using Argon gas (see Fig. 16).



Figure 15: SEM Zeiss DSM 982 GEMINI

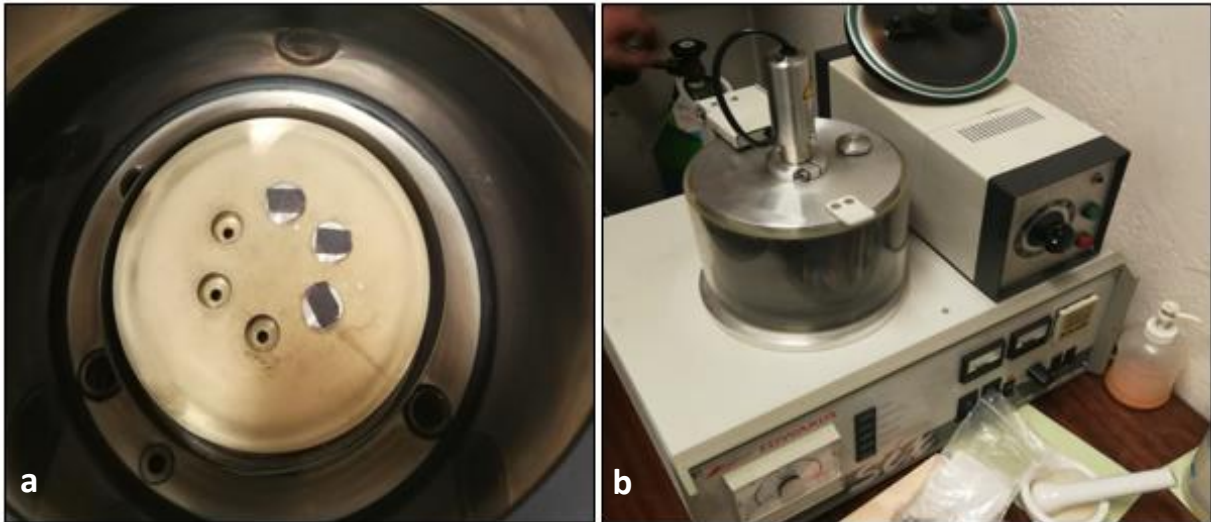


Figure 16: a: gold/paladium layer on the samples after coating. b: vacuum chamber of the coating device.

The scanning-electron-microscope used for the investigations (Zeiss DSM 982 GEMINI) is located at the Karl-Franzens University of Graz (Fig. 15).

In order to analyse the first stages of the hydration process with the SEM, the hydration of the samples was stopped after 10 minutes and 3 hours. 3 cement mixes were analysed: mix 1, mix 3 and mix 4 (tab. 7 and 9). To stop the hydration after 10 minutes and 3 hours the cement was placed on a 90 mm diameter cellulose filter on a porcelain funnel. Samples stopped after 3 hours had to be crushed first because they were already hard. Then isopropanol was poured over the sample in order to remove the water from the sample by solvent exchange (Fig. 17). With the help of a vacuum in the bottle connected to the funnel, the isopropanol and the water got extracted through the filter. After this process, the sample was placed into a light-vacuum (300 mbar) chamber for at least 1 day to get rid of the remaining isopropanol. After that the sample was stored in an airtight container to avoid contact with the atmosphere.



Figure 17: CEM I reference mix on the cellulose filter after the addition of isopropanol. Glass container underneath is under vacuum.

2.4. Real scale tests

During the 22nd -26th of July 2019 real scale dry-mix shotcrete tests were carried out in Wopfing, Lower Austria, where the company “BAUMIT” has its headquarter as well as the installations and equipment for dry-mix shotcrete spraying and testing. 14 different shotcrete mixes, each consisting of 400 kg aggregate with 64 kg binder were sprayed and analysed. Water/cement ratio changed for every application due to the nozzle man’s own assessment of the shotcrete consistency. At the BAUMIT innovation centre the spraying equipment was placed inside two containers, separating the mixing device and water pumping system in one container (Fig. 18a) from the actual spraying application in the other container (Fig. 18b). An experienced nozzle-operator sprayed the shotcrete in wooden boxes placed on the floor and supported on a wall allowing perpendicular spraying on the surface (see figure 18b).



Figure 18: a: Mixing device in one of the containers in Wopfing. b: Wooden boxes, where the shotcrete was sprayed and red nozzle of the spraying device.

The early compressive strength of the shotcrete was measured by means of a penetration needle (from 0.2 to 1 MPa), and with a DX 450-SCT powder-activated testing device from Hilti equipped with threaded studs (from 2 to 16 MPa), according to EN 14488-2 (Austrian Society for Construction Technology. 2013).

Additionally, drill cores were taken to test the compressive strength after 28 and 90 days.

2.4.1. Needle Penetration test

The apparatus consists of a spring penetrometer (Proctor-penetrometer) and a stainless-steel needle pointer (Fig. 19). A sliding ring indicates the reached load on the handle of the penetrometer (in N). The needle penetrates the sprayed concrete to a depth of 15 mm during the first few hours after application. Ten readings are taken at each measurement time. The values obtained are then 'converted' to compressive strength according to ÖNORM EN 14488-2 (Fig. 20). The penetration test is used for measuring strength between 0.2 and 1 MPa.



Figure 19: Needle Penetration Test carried out in Wopfung

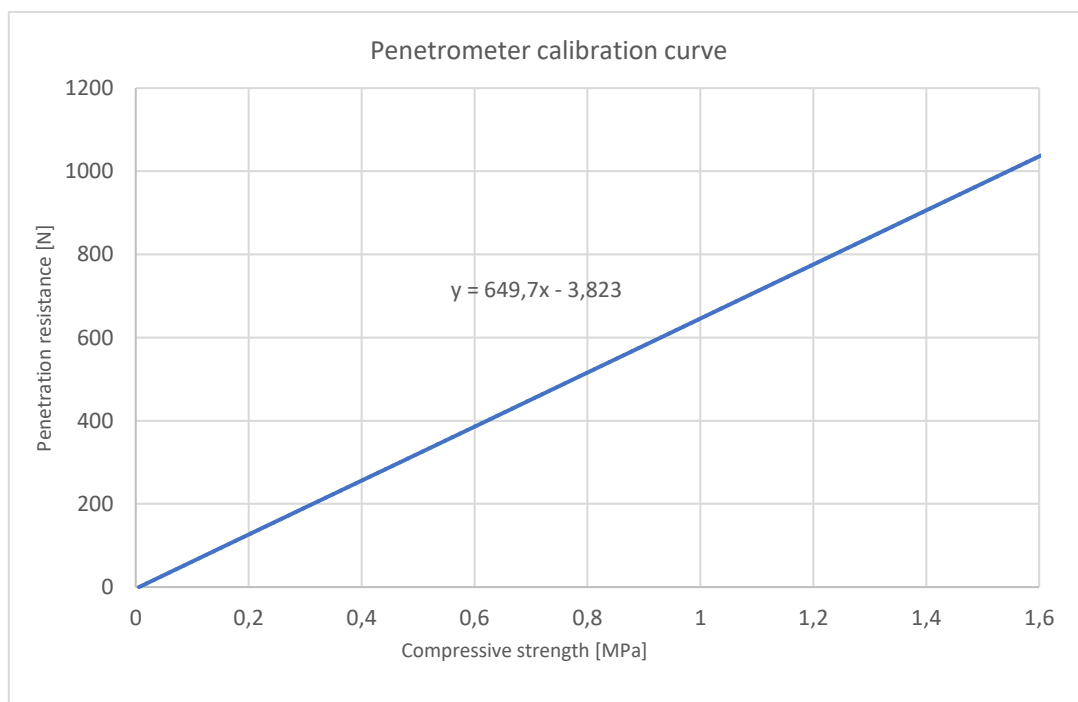


Figure 20: Calibration curve (ÖNORM EN 14488-2)

2.4.2. Stud driving method

Threaded studs are used to determine compressive strengths between 2 and 16 MPa. The Hilti DX 450-SCT with green cartridges is the recommended measurement tool that drives the studs into the shotcrete surface (Fig. 21). Six to ten readings are necessary to get accurate



Figure 21: Stud driving test carried out in Wopfing

results. Three different sizes of studs are used, depending on the strength of the concrete and thus on the depth of penetration. The studs must achieve a penetration depth of at least 20 mm and should be distanced from each other by 80 mm. Before pulling them out, the remaining length of the studs is noted. By using the HILTI Tester 4 the pulling out force is determined. The ratio between the length of the studs (“L”) and the pulling out force (“F”) is matched with the calibration curve (Fig. 22) resulting in the compressive strength of the shotcrete.

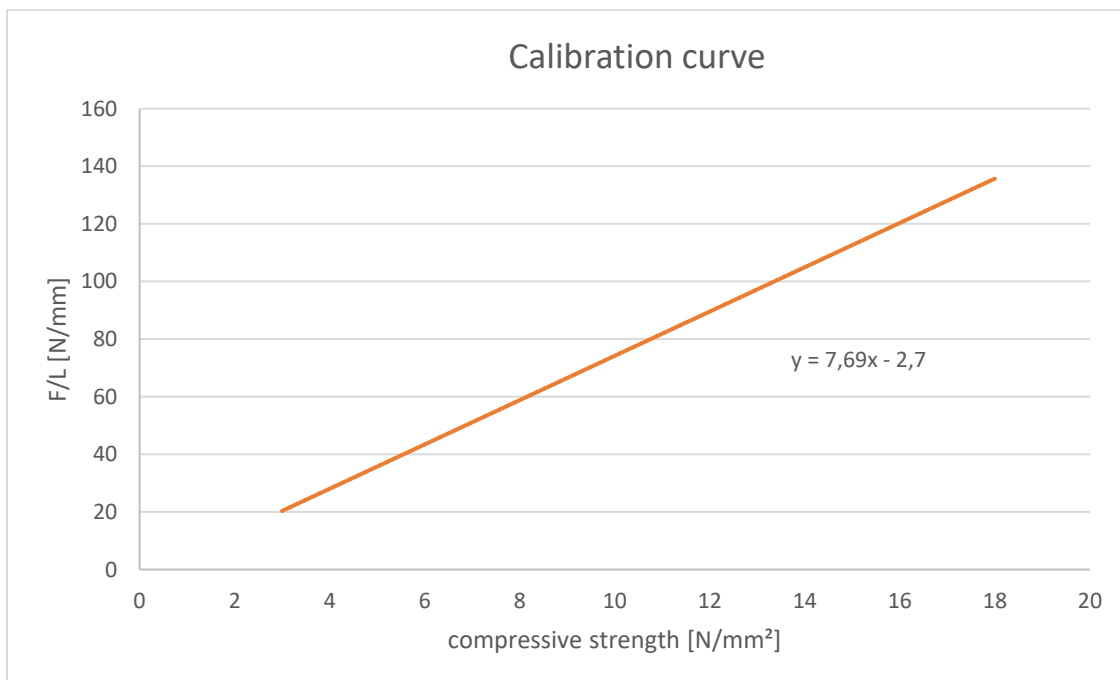


Figure 22: calibration curve of the stud driving method (ÖNORM EN 14488-2)

2.4.3. Drill cores and compressive strength

Drill cores were used to test compressive strength of the shotcrete after 28 and 90 days (Fig. 23). Diameter of the drill cores was 100 mm and the height at least 200 mm. Before testing, the cores were stored under water according to ÖNORM EN 12390-2. The test plant L. Kissling&Co. VPC-21 was used to determine the compressive strength of the drill cores. The maximum load of this machine is 1500 kN.



Figure 23: Drill machine used in Wopfing

3. Results

Table 9 shows which laboratory test method was performed for the different mixes. The different components of each mix are shown in table 7. Mixes 3 and 4 were also tested in real scale samples (mixes P11a and P14, respectively); in those samples early and late strength was measured.

Table 9: List of the different methods used to analyse the lab mixes. Positive visual tests are highlighted green.

Sample	Visual test	Calorimeter	XRD	Compressive strength test	Flexural strength test	SEM	Real scale test
Mix 1	x	x	x			x	
Mix 2	x	x	x				
Mix 3	x	x	x	x	x	x	x
Mix 4	x	x	x	x	x	x	x
Mix 5	x		x				
Mix 6	x	x					
Mix 7	x	x					
Mix 8	x	x					
Mix 9	x	x					
Mix 10	x	x					
Mix 11	x	x					
Mix 12	x	x					
Mix 13	x	x					
Mix 14	x	x					
Mix 15	x	x		x	x		
Mix 16	x	x					
Mix 17	x						
Mix 18	x	x					
Mix 19	x	x					
Mix 20	x	x					
Mix 21	x						
Mix 22	x						

3.1. Laboratory results

3.1.1. Visual tests

From all the mixes presented in table 7, only mixes 3, 4, 5, and 15 showed fast setting, under 2 minutes. Mixes 3 and 4 showed 'ideal' setting time, ~1 minute. Mix 5 hardened too fast, in less than 30 seconds, and was then not considered suitable for shotcrete and thus no further tests were performed with this mix, similarly to the rest of the mixes where the setting took longer than 2 minutes. Only mixes 3, 4 and 15 passed the first visual test and were selected for strength tests.

3.1.2. Isothermal calorimetric analyses

Figures 24-26 show the calorimetry curves of mixes 1, 2, 3 and 4 from table 7. Mix 3 reaches the highest heat flux value in the first couple of minutes of hydration, about 40% higher than mixes 1 and 4 (Fig. 24). In the case of mix 2, the highest heat value in this early hydration period is 70-80% lower than in mixes 1 and 4. As explained in the 'Experimental' section, the first exothermic peak is mainly attributed to the dissolution heat and that evolved from the early formation of ettringite. The lowest heat evolved from mix 2 in this period agrees well with the XRD results (see section 3.1.3.) which show no ettringite formation in the first minutes. It is worth noting that this first calorimetry peak does not include all heat generated since the water was added to the binder because the samples were externally mixed.

After the induction period, the heat flux starts to rise again after 3 h in mixes 1, 3 and 4, as a result of the silicate reaction and C-S-H formation (Fig.25). The heat evolved from this reaction in mix 4, with 20% slag, is slightly lower than that in mixes 1 and 3. The maximum values reached are 4.8 and 4.3 mW/g for mixes 3 and 4, respectively. Mix 2 shows a different heat flow curve, including a little bump after 2-3 h and a small peak between 8 and 14 h. From the 15th hour onwards the heat increases considerably, reaching a maximum of around 7.4 mW/g after 21 hours. These reactions are attributed to the formation of monosulfoaluminate and dicalcium silicate reaction.

Figure 26 shows the cumulative heat curves of the 4 samples mentioned. Mixes 1 and 3 reach the highest cumulative heat after 24 hours, ~250 J/g cement. Despite the slower increase of the cumulative heat up to the 18th hour, mix 2 reaches similar values to mix 4 after 24 hours.

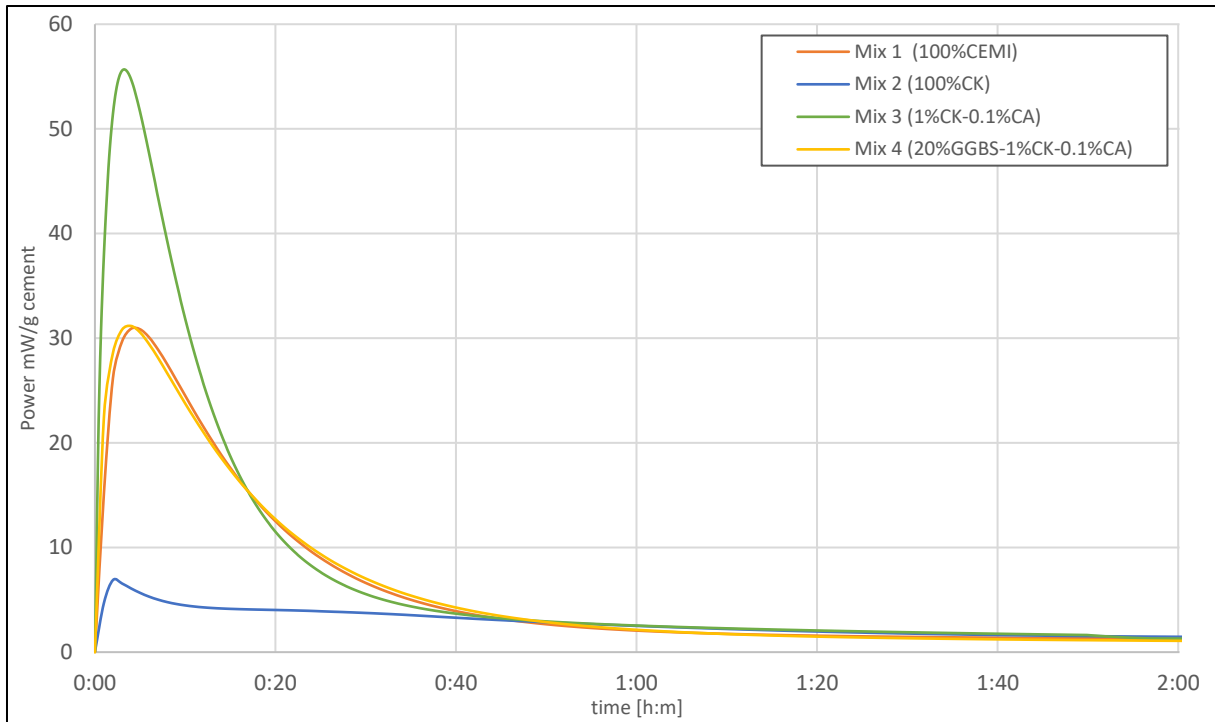


Figure 24: Heat flux of mixes 1(100%CEMI), 2(100%CK), 3(1%CK-0.1%CA) and 4(20%GGBS-1%CK-0.1%CA) after 2h of hydration.

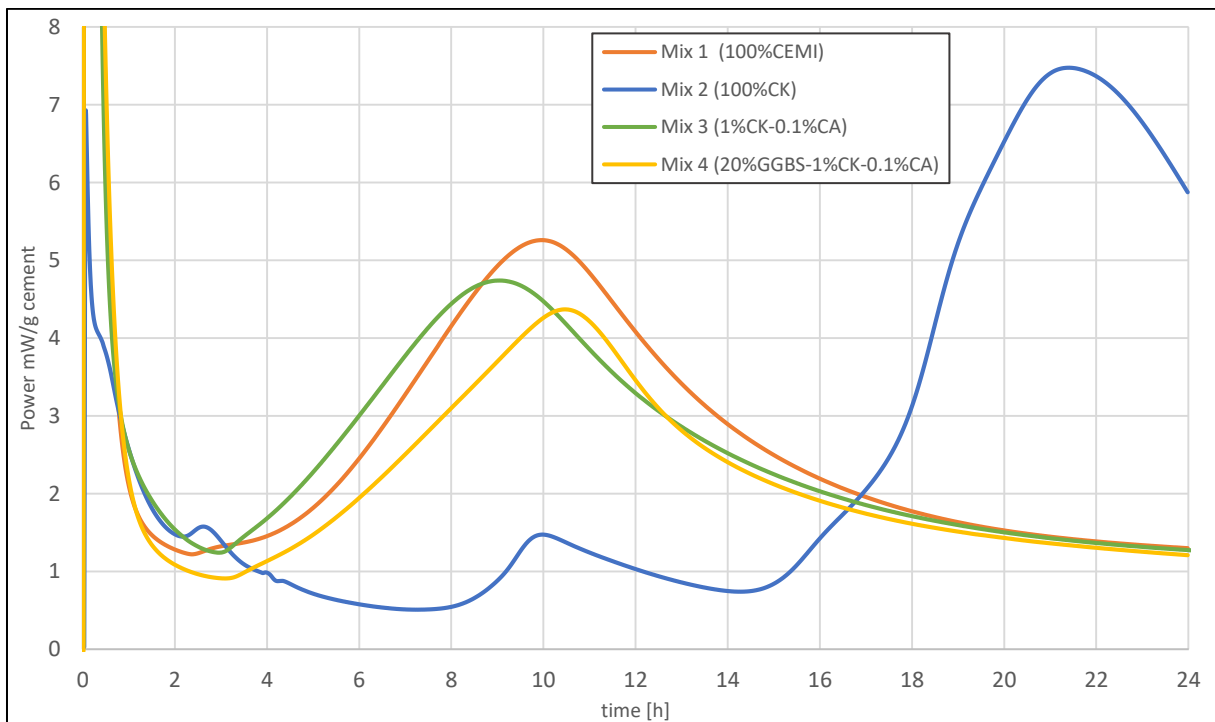


Figure 25: Heat flux of mixes 1(100%CEMI), 2(100%CK), 3(1%CK-0.1%CA) and 4(20%GGBS-1%CK-0.1%CA) after 24h of hydration.

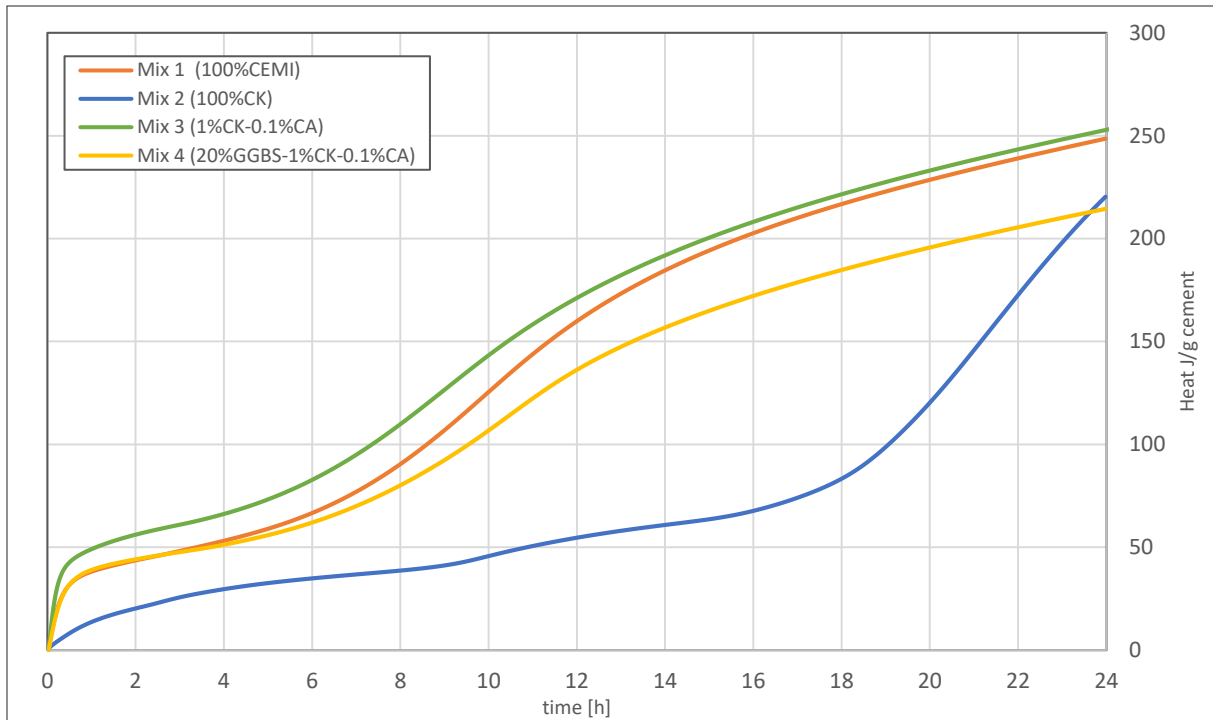


Figure 26: Cumulative heat of mixes 1(100%CEMI), 2(100%CK), 3(1%CK-0.1%CA) and 4(20%GGBS-1%CK-0.1%CA) after 24h of hydration.

Figures 27-29 show the calorimetry curves of various CEM-CSA(Alpenat CK) mixes with different CSA contents, from 1 to 40% (Mixes 3, 6, 7, 8 and 15 from table 7). The mixes containing 20, 30 and 40% CSA (mixes 8, 7 and 6, respectively) show a very high heat development in the first couple of minutes, higher than 58 mW/g cement. The maximum heat reached by these 3 mixes was actually higher than the detection limit of the equipment (1.1 W) and this is why the peaks are not complete in the graph. After this initial hydration stage, the heat curves of mixes 7 and 8 do not rise again; they actually decrease continuously over time up to the 24th h. Mix 6 starts to rise again after 21 h (Fig. 28). Mix 15, with 5% CSA, shows a very similar heat development to mix 3, with 1% CSA. The maximum value reached during the silicate reaction of mix 15, around the 7th hour, is slightly lower 4 mW/g, than that from mix 3, 4.8 mW/g, reached around the 9th hour.

Mixes with 1 and 5% CSA reach the highest cumulative heat, 250 J/g cement. Samples with 20% CSA or higher reach 50% lower values (Fig. 29). The fact that the detection limit was reached by mix 6, 7 and 8 must be taken into consideration when analysing the cumulative heat results.

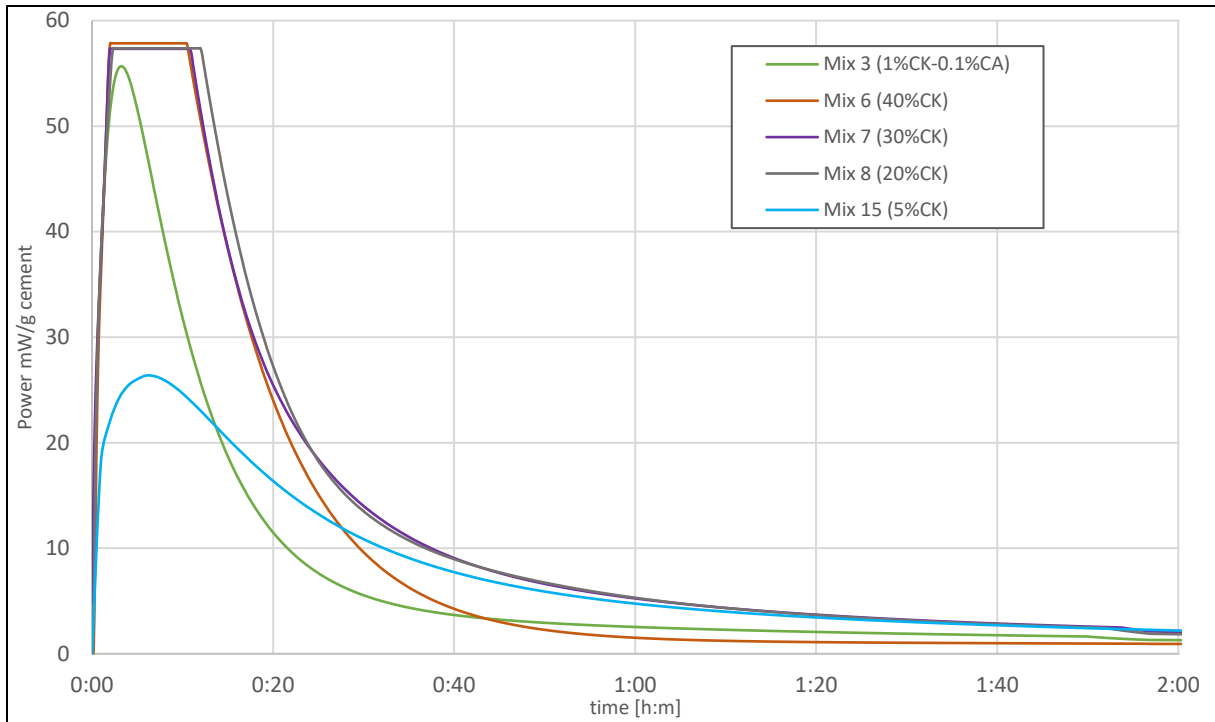


Figure 27: Heat flux of mixes 3(1%CK-0.1%CA), 6(40%CK), 7(30%CK), 8(20%CK), 15(5%CK) after 2h of hydration.

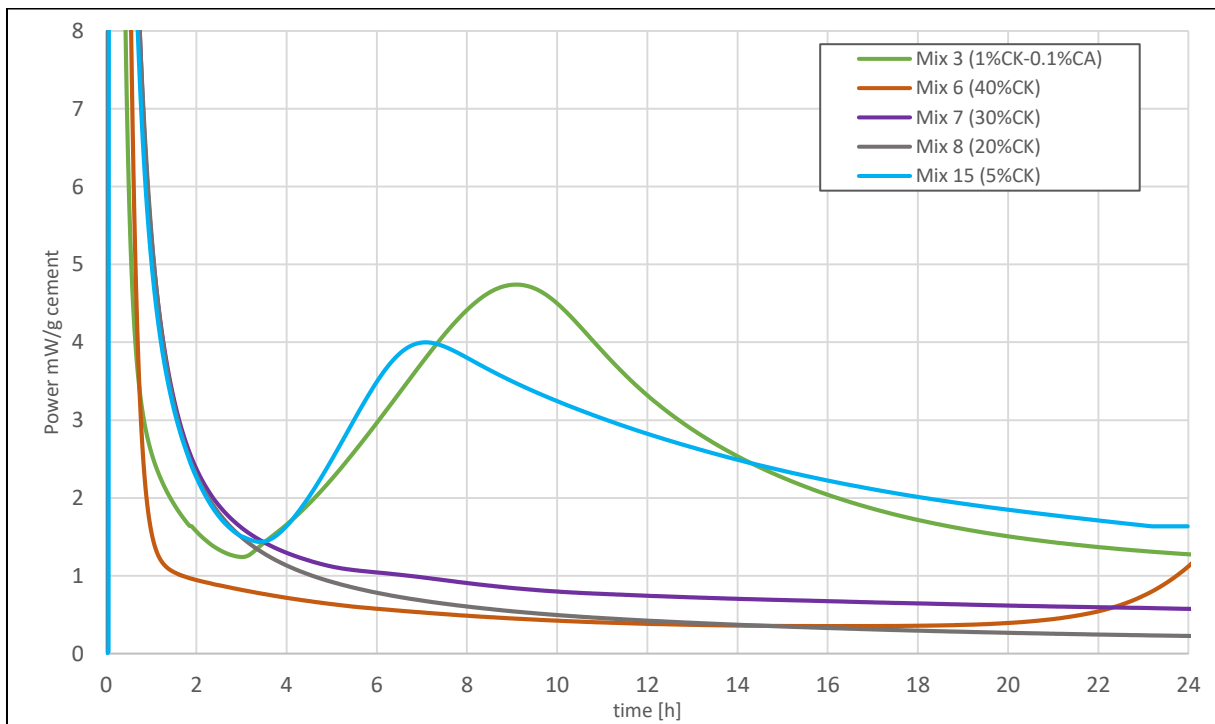


Figure 28: Heat flux of mixes 3(1%CK-0.1%CA), 6(40%CK), 7(30%CK), 8(20%CK), 15(5%CK) after 24h of hydration.

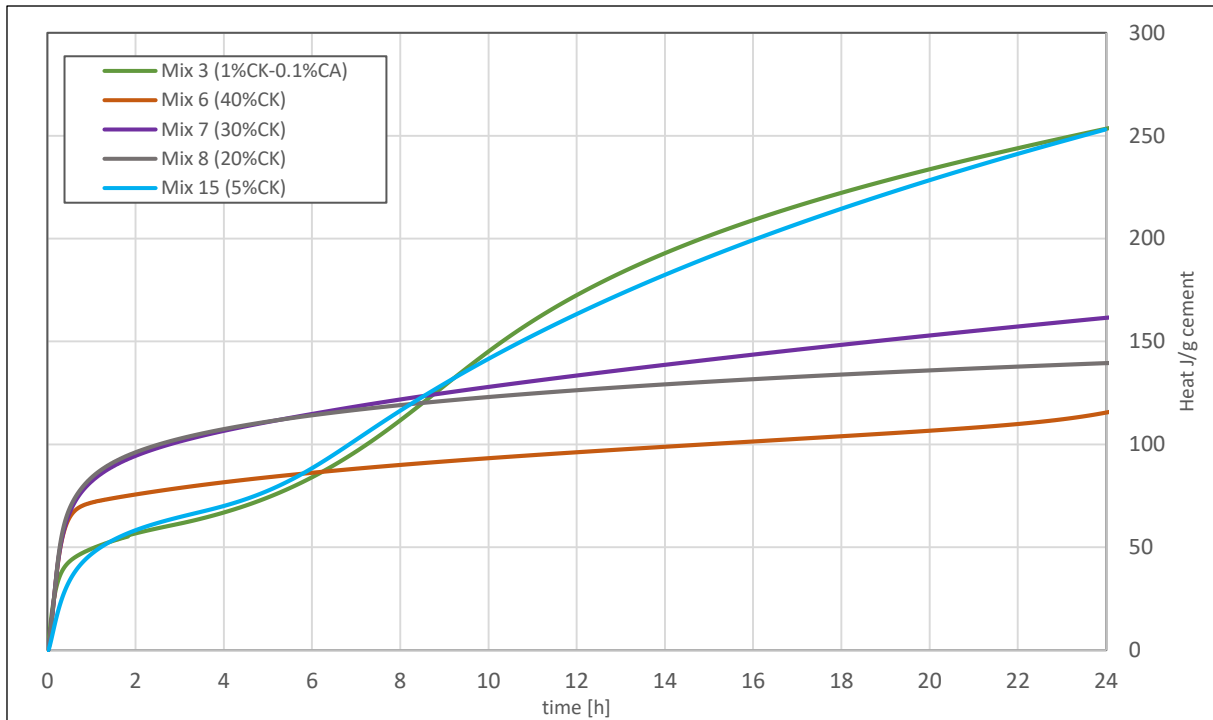


Figure 29: Cumulative heat of mixes 3(1%CK-0.1%CA), 6(40%CK), 7(30%CK), 8(20%CK), 15(5%CK) after 24h of hydration.

Even though the ‘visual’ tests did not show good results for mixes with SR0 cement, calorimetry tests were performed for further analysis and understanding. Figures 30, 31 and 32 show 5 different mixes containing SR0 and CSA (Mixes 10, 11, 12, 13, 14 (without CSA) from table 7). Comparing these curves with those from the CEM I samples (Figs. 27, 28 and 29), it can be appreciated that the heat flux at the beginning is about 50% lower in the SR0 mixes, which only reach ~ 27 mW/g. In the case of mix 10, with 50% SR0 and 50% CK, the detection limit was reached and the heat evolved in these first minutes is thus not fully included. In mixes 10 and 11 the heat keeps decreasing from the first peak maximum until the end of the test, no silicate reaction is observed. Mix 13 with 0.5% $\text{Ca}(\text{OH})_2$ reaches the lowest initial heat values but then it starts to increase after 2 h, following a very similar behaviour as Mix 14 with 100% SR0. Also mix 12, with 90%SR0-10%R2, shows a silicate reaction starting after 2 hours and reaching its maximum after around 8 hours. In the 3 mixes that showed silicate reaction, mixes 12, 13 and 14, the maximum values did not reach 4 mW/g. The cumulative heat of these 3 mixes (Fig. 32) reached similar values after 24 hours, 220 J/g, up to 4 times higher than the other two mixes (Mixes 10 and 11). The fact that the detection limit was reached by mix 10 must be taken into consideration when analysing the cumulative heat results.

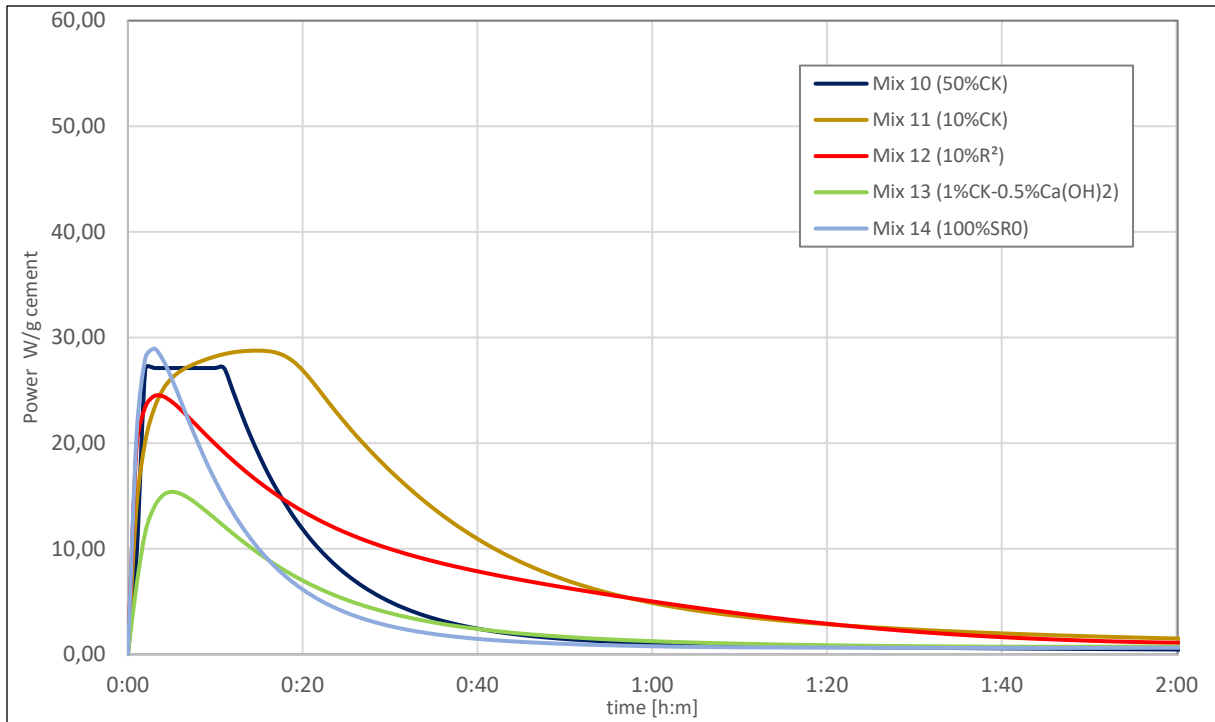


Figure 30: Heat flux of mixes 10(50%CK), 11(10%CK), 12(10%R²), 13(1%CK-0.5%Ca(OH)₂) and 14(100%SR0) after 2h of hydration.

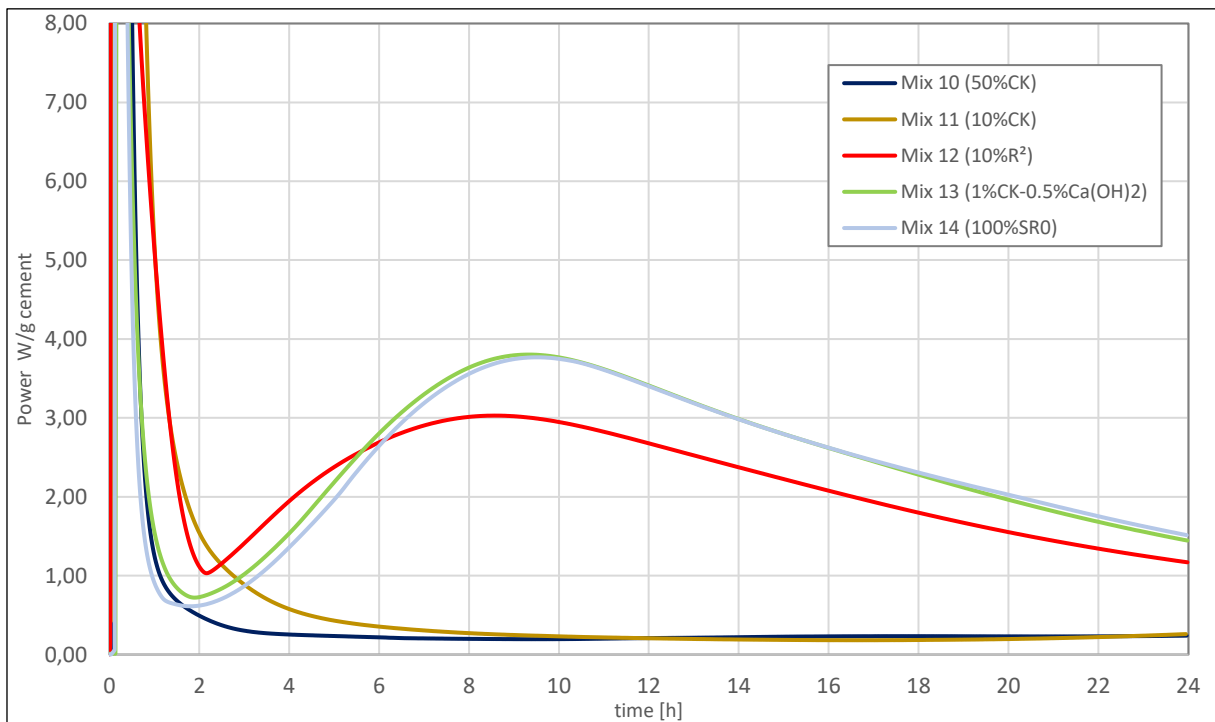


Figure 31: Heat flux of mixes 10(50%CK), 11(10%CK), 12(10%R²), 13(0.1%CK-0.5%Ca(OH)₂) and 14(100%SR0) after 24h of hydration.

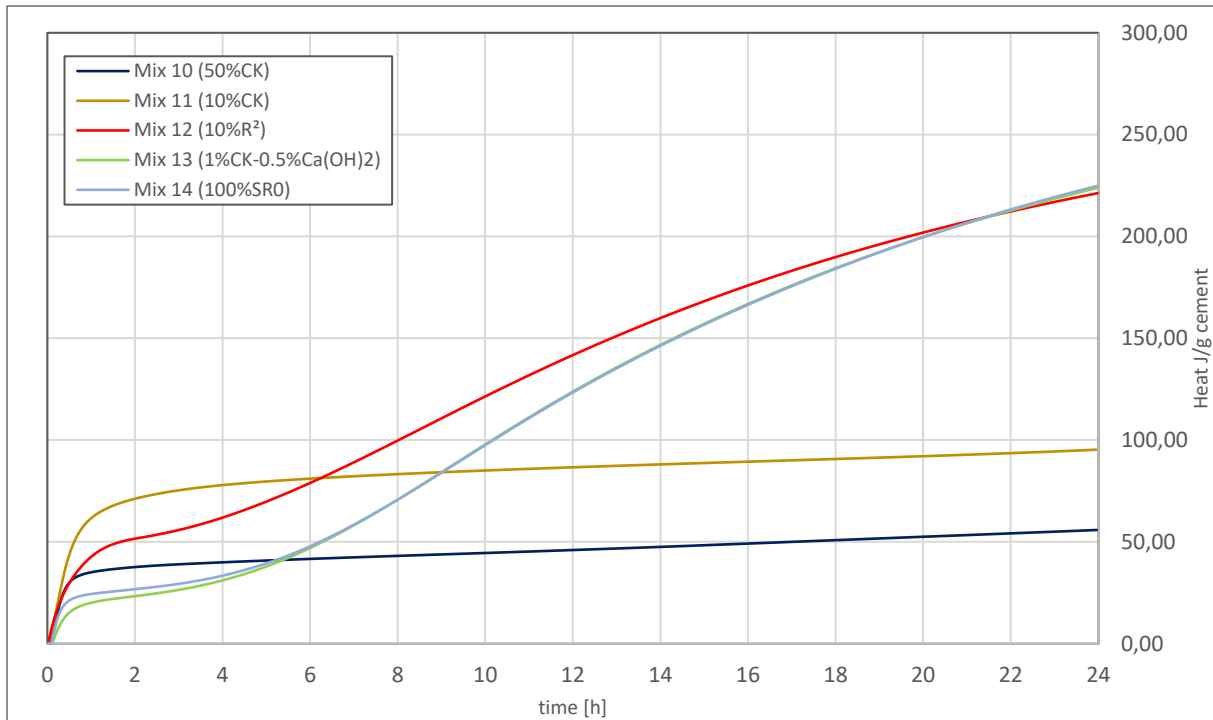


Figure 32: Cumulative heat of mixes 10(50%CK), 11(10%CK), 12(10%R²), 13(0.1%CK-0.5%Ca(OH)₂) and 14(100%SR0) after 24h of hydration.

3.1.3. XRD-measurements

The following figures (fig. 33 – 37) present the 24 hour in-situ XRD measurements of mixes 1, 2, 3, 4 and 5 with scans displayed every 30 minutes. The whole set of patterns can be found in the Appendix. The reference sample mix 1 (100% CEM I) (Fig. 33) shows ettringite early formation in the first 15 minutes, reaching its maximum after 2 hours, and decreasing slightly thereafter (~10.5°). Portlandite peak intensity (~21°) remains very small and only significant from the 18th hour onwards. Anhydrite peak intensity (~29.5°) decreases over time and is consumed after 17 h.

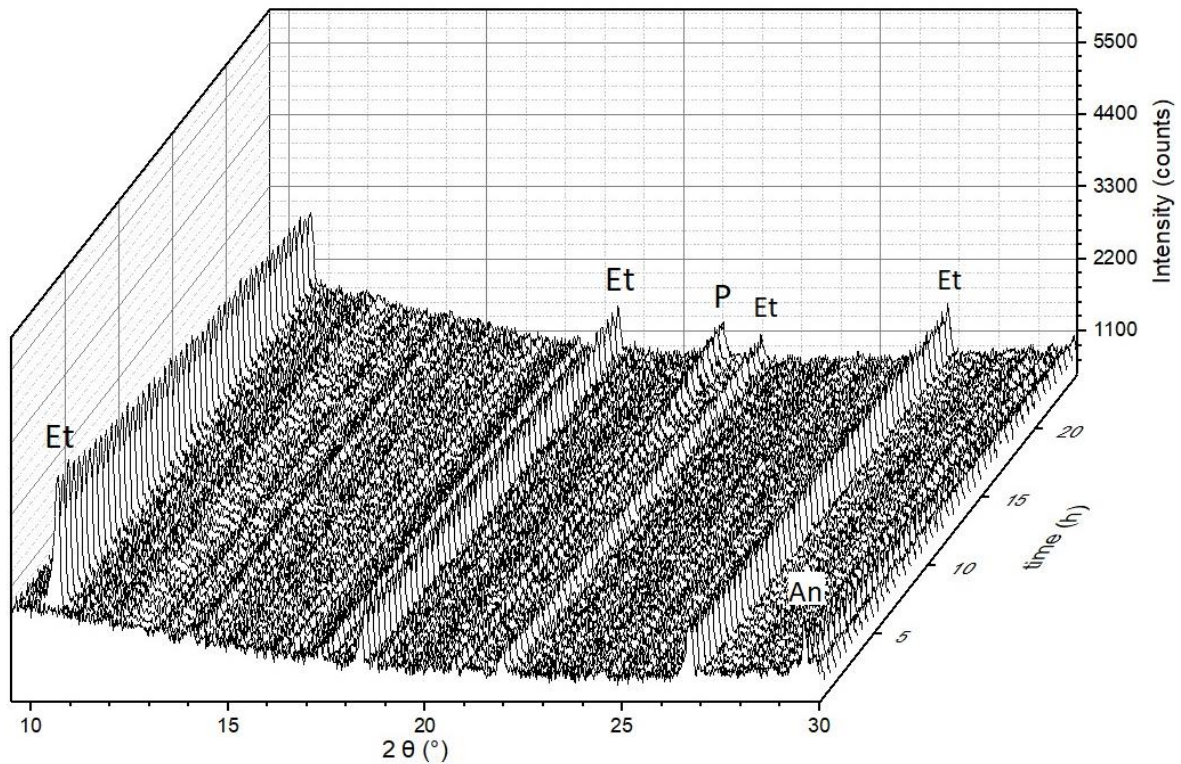


Figure 33: XRD- scans (every 30 minutes) from 9-30° 2 θ of mix 1 up to 24h (Et=ettringite, P=portlandite, An=anhydrite)

Figure 34 shows the first 24 h of hydration of the reference sample mix 2 (100% CSA). In the first hours of hydration the ye'elemite peak ($\sim 27^\circ$) is dominant but it starts to decline once ettringite ($\sim 10.5^\circ$) starts to form, after 4 h, together with the decrease of anhydrite ($\sim 48.5^\circ$). Between 25° and 40° 2theta a broad bump is observed at early stages of hydration during which the samples were still very fluid (Fig. 50 appendix). Due to the very high peaks of ye'elemite, the y-axis of figure 34 is displayed up to 10500 counts.

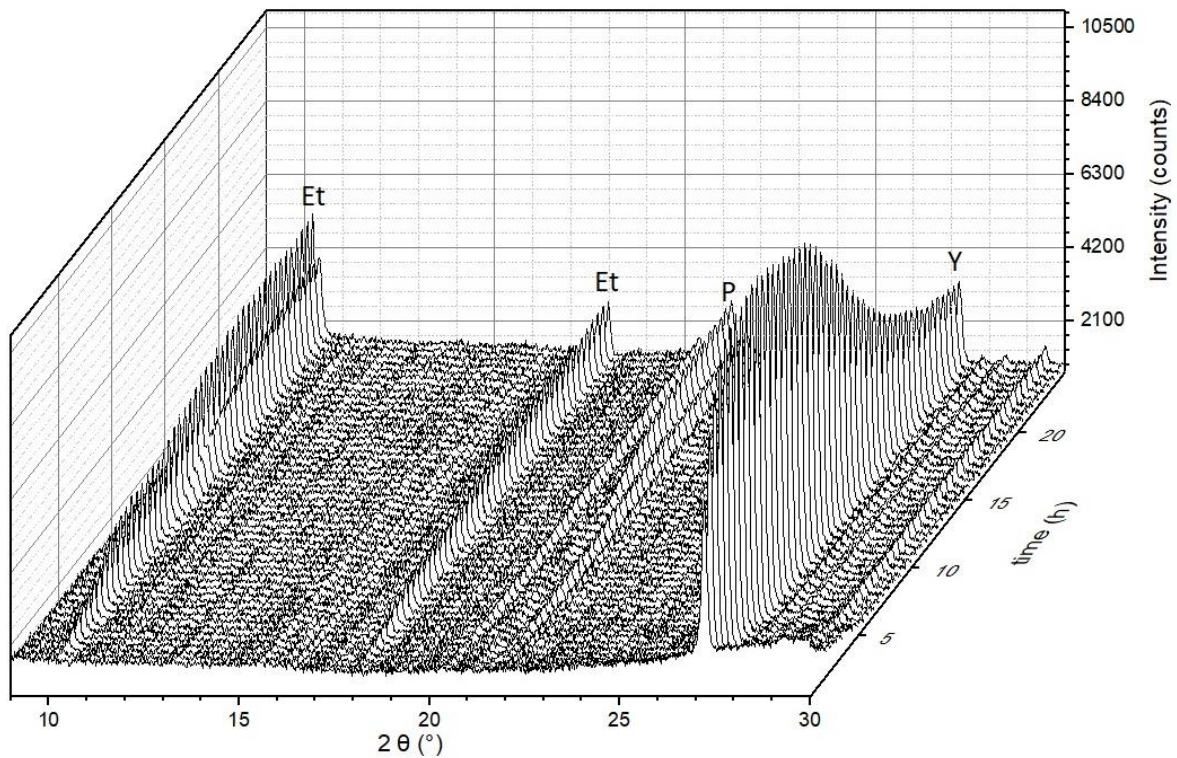


Figure 34: XRD- scans (every 30 minutes) from 9-30° 2θ of mix 2 up to 24h (Et=ettringite, P=portlandite, Y= ye'elemite)

The XRD patterns of sample mix 3 (Fig. 35) show the formation of ettringite ($\sim 10.5^\circ$) starting immediately after mixing and reaching its maximum after 12 h. Monosulfate ($\sim 12^\circ$) is also present from the beginning of hydration, maintaining a consistent broad peak throughout the first 24 h. Portlandite ($\sim 21^\circ$) starts to form after 11 h and keeps increasing. Anhydrite ($\sim 29.5^\circ$) is only present in the first 4 h of hydration. Comparing this sample with mix 1, the main difference is the instant formation of ettringite and monosulfate in mix 3, even though the intensity of ettringite peaks is much lower than in the reference sample (mix 1). Additionally, portlandite develops considerably higher peaks in mix 3 than in mix 1.

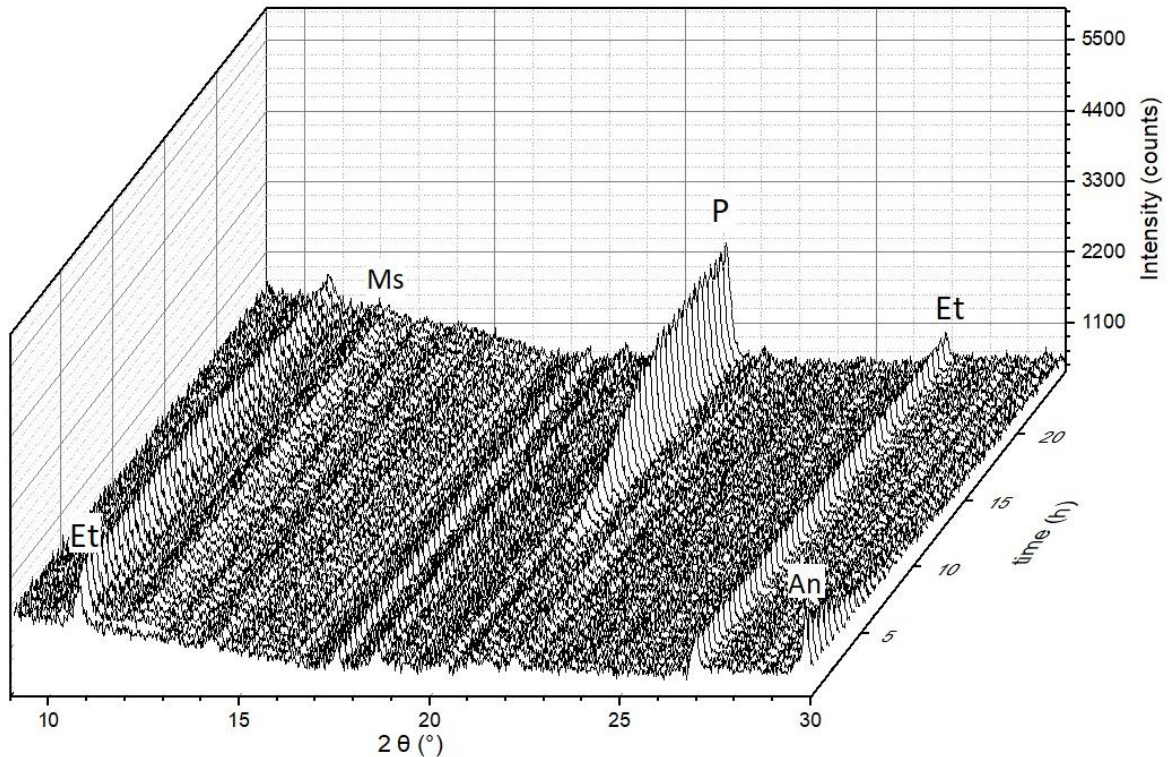


Figure 35: XRD- scans (every 30 minutes) from 9-30° 2θ of mix 3 up to 24h (Et=ettringite, Ms=monosulfate, P=portlandite, An=anhydrite)

The influence of blast furnace slag in the PC-CSA mix is shown in figure 36. Since this mix contains less Portland cement (CEMI), the peaks from the anhydrous cement phases are expected to be smaller throughout all patterns than those in figure 35. For better display of the scans, the y-axis in figure 36 is smaller (3000 counts). Ettringite ($\sim 10.5^\circ$) reaches its maximum after 15 h and slowly decreases afterwards. The formation of portlandite ($\sim 21^\circ$) starts after ~ 7 h. The biggest difference compared to mix 3 is the up to 50% lower intensity of all peaks.

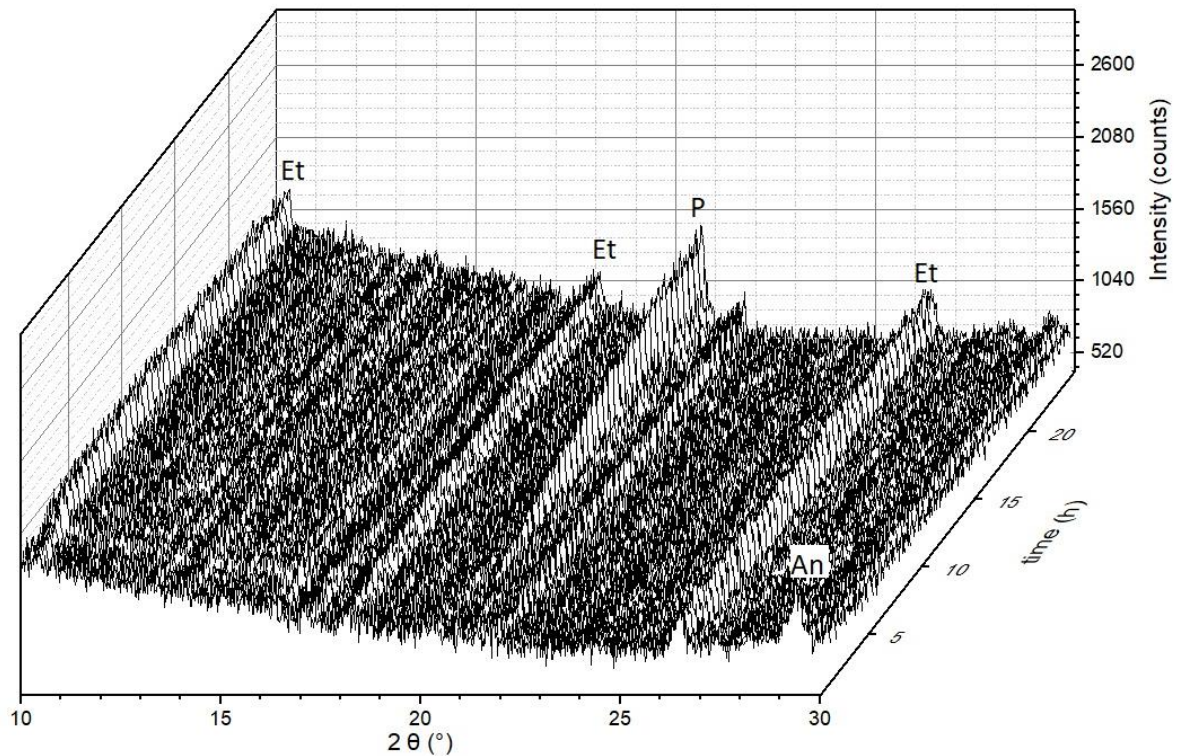


Figure 36: XRD- scans (every 30 minutes) from 9-30° 2θ of mix 4 up to 24h (Et=ettringite, P=portlandite, An=anhydrite)

The influence of citric acid can be assessed by comparing mix 3 sample (Fig. 35) with mix 5 sample (Fig. 37). The formation of ettringite ($\sim 10.5^\circ$) is slower in the mix without citric acid, showing only very small peaks in the first hour and reaching its maximum after 15 h. However, the ettringite peaks show higher intensities from the 4th hour on and up to the 24th, and no monosulfate peak is visible in the sample without citric acid. Alite decrease can be detected from the 5th h onwards (Fig. 53 appendix), and the peaks decline faster than those in the sample with citric acid. Portlandite peaks have lower intensities than in mix 3.

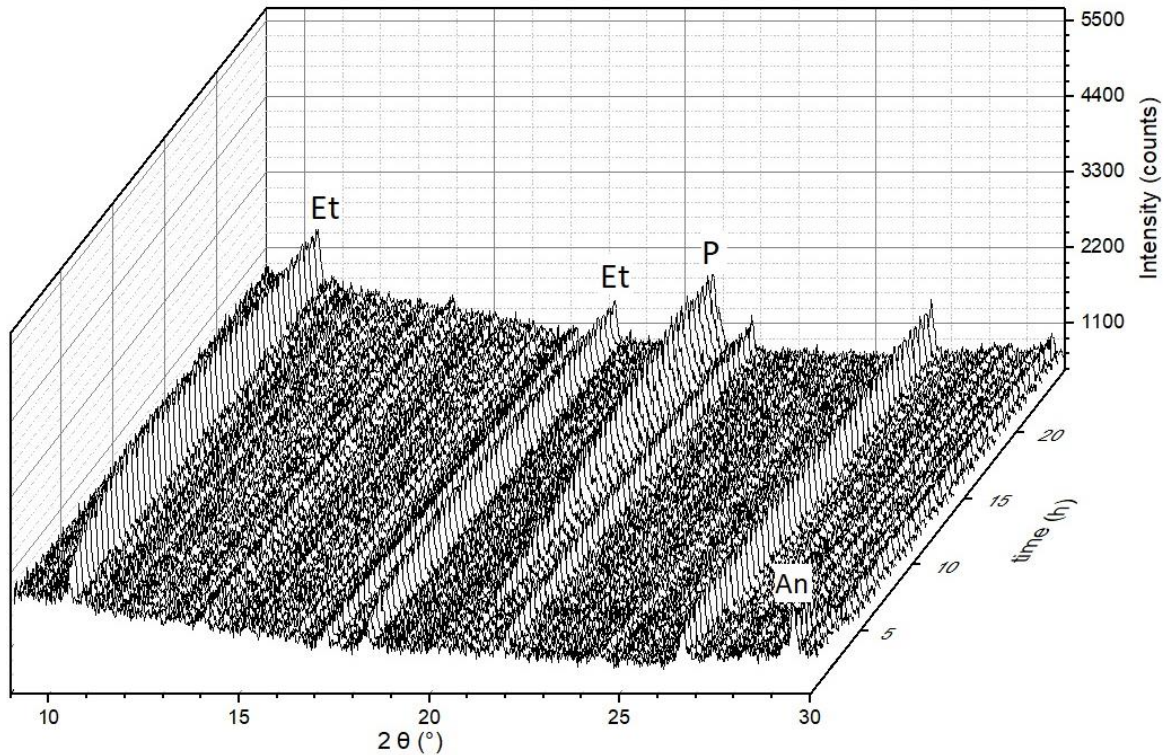


Figure 37: XRD- scans (every 30 minutes) from $9\text{--}30^\circ 2\theta$ of mix 5 up to 24h (Et=ettringite, P=portlandite, An=anhydrite)

Figure 38 shows the single XRD-measurements of mixes 3 and 4, which have the same binder composition except for the 20% slag in mix 4, after 14 days of hydration. Portlandite formation ($\sim 20^\circ$, $\sim 40^\circ$) is dominant, and alite ($\sim 37^\circ$) is almost depleted. Furthermore, the presence of monosulfate ($\sim 12.5^\circ$) after 14 days is very notable. The biggest difference between both scans is the higher background intensity in the region between $\sim 25^\circ$ and $\sim 45^\circ$ 2θ in the slag sample, Mix 4, which corresponds to a higher amorphous contribution of the C-S-H to the pattern.

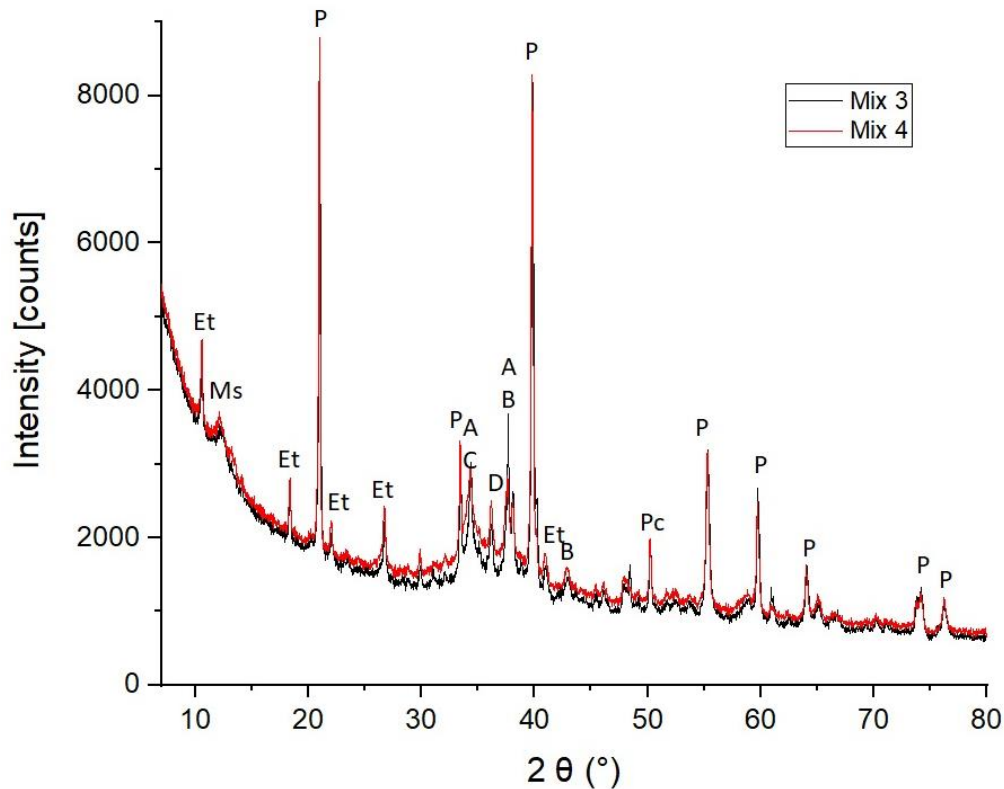


Figure 38: XRD-patterns of mix 3 and mix 4 from 7-80° 2θ measured 14 days after hydrating the cement (Et=ettringite, Ms=monosulfate, P=portlandite, A=alite, B=belite, C=calcite, D=dolomite, Pc=periclase)

3.1.4. Compressive/flexural strength

Compressive and flexural strength measurements were carried out on the 3 mixes that passed the visual tests: mixes 3, 4 and 15. Mix 15 broke apart without detecting any measurements after 6h. After 24 h mix 15 reached a compressive strength of 2.1 N/mm². The other two mixes showed higher results, the biggest differences occurring after 24 h, when mix 3 showed twice as much compressive strength than mix 4, with GGBS (Fig. 39). After 28 and 100 days, however, mix 4 prisms showed slightly higher strength values.

The flexural strength values showed a similar trend as the compressive strength in the first 24 h, mix 3 reaching values almost two times higher than mix 4 (Fig. 40). After 28 days mix 3 still shows slightly higher values than mix 4, and after 100 days both mixes reach very similar flexural strength values.

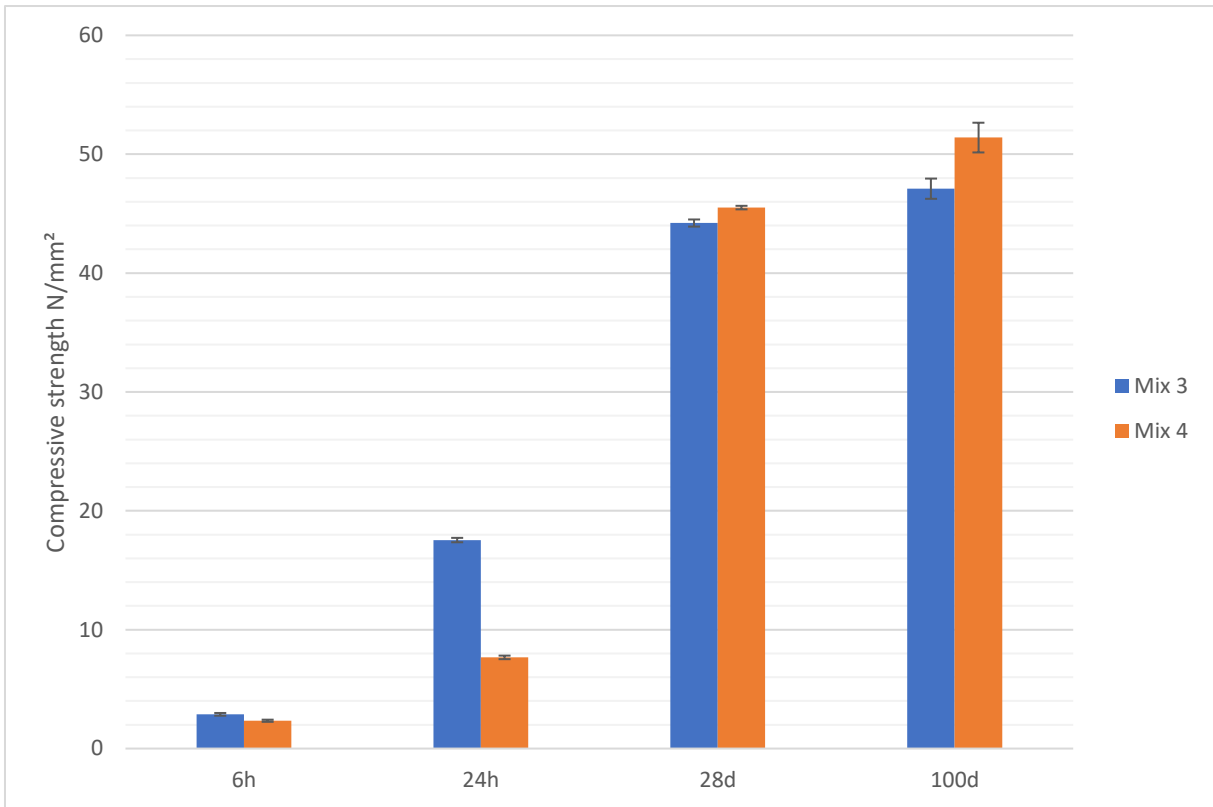


Figure 39: Compressive strength results of mix 3 and 4 up to 100 days

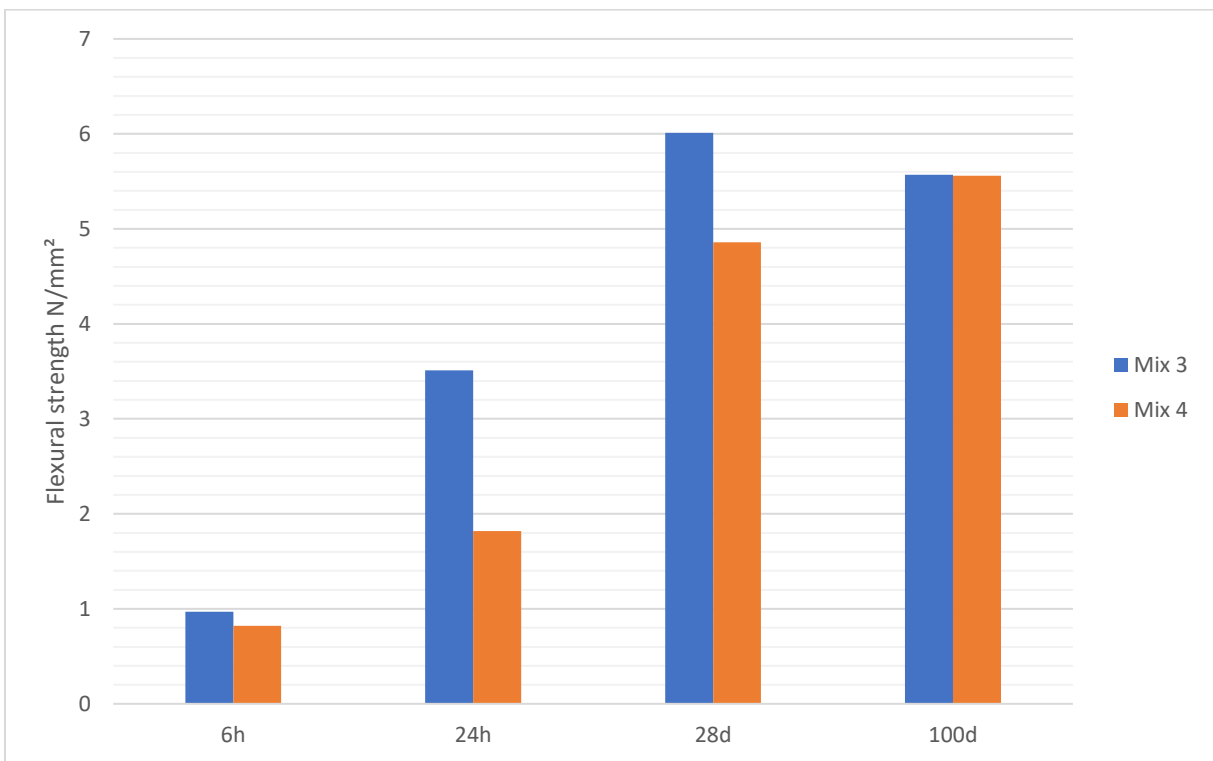


Figure 40: Flexural strength results of mix 3 and 4 up to 100 days

3.1.5. SEM results

As explained before, the hydration process of mixes 1, 3 and 4 was stopped after 10 min and 3 h in order to analyse the morphological properties by means of scanning electron microscopy. Figure 41 shows the reference sample (mix 1 with 100% CEM I) after 10 minutes hydration. Using a magnification of 15000x, small ettringite needles (< 1 μm) as well as some amorphous hydrates can be observed on the surface of a cement grain.

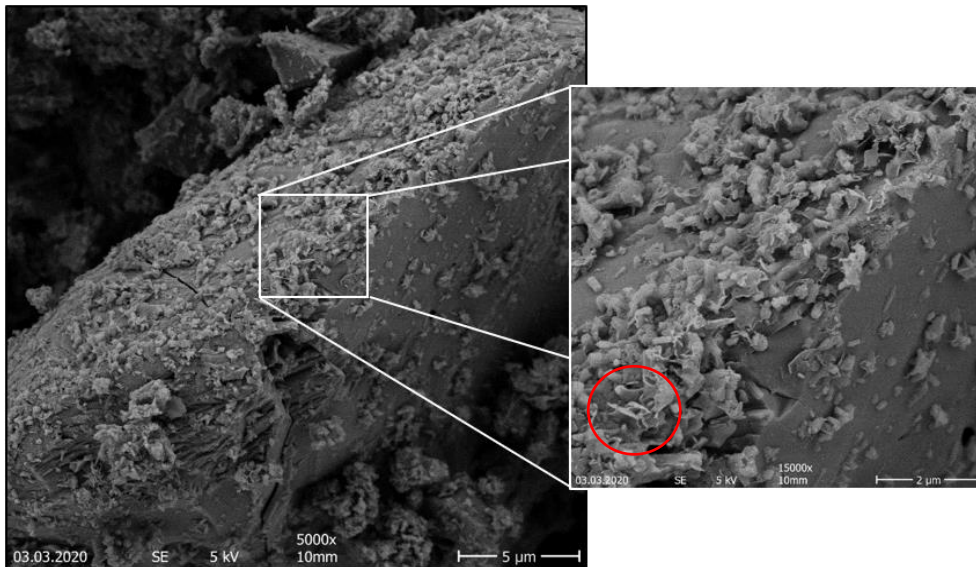


Figure 41: Mix 1, after 10 minutes hydration, small ettringite needles in the red circle

SEM pictures of mix 3 after 10 minutes (Fig. 42) show a higher hydration degree than in mix 1. The whole surface of the cement grain of mix 3 is covered with hydrated phases, with various morphologies and crystallinities. Ettringite needles reach in this sample sizes of 1 μm .

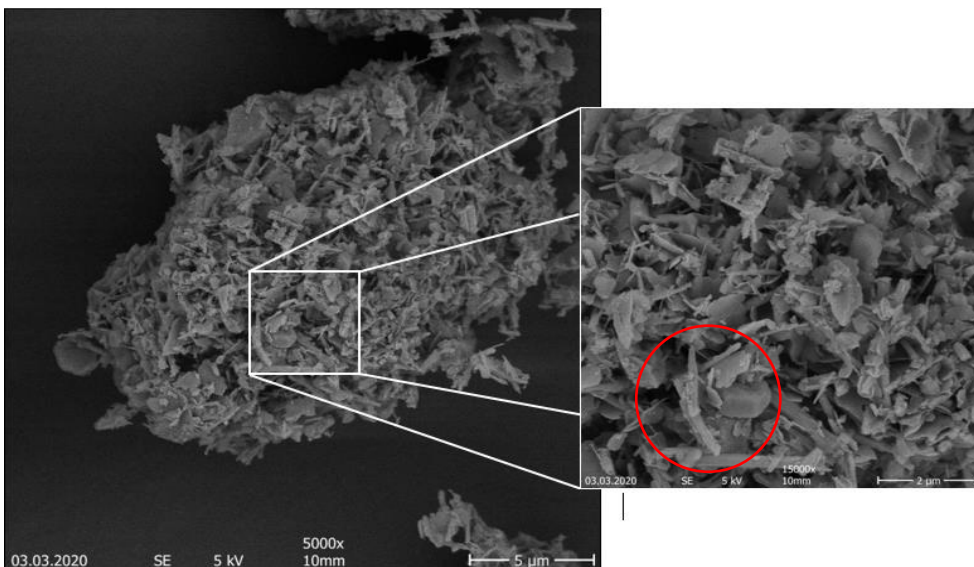


Figure 42: Mix 3, after 10 minutes hydration, ettringite needles in the red circle

Similar to mix 3, mix 4 shows cement grains surfaces completely covered with hydrated phases (Fig. 43). Some ettringite needles can be seen, but mostly the surface is covered by AFm plates, with sizes of 1-2 μm .

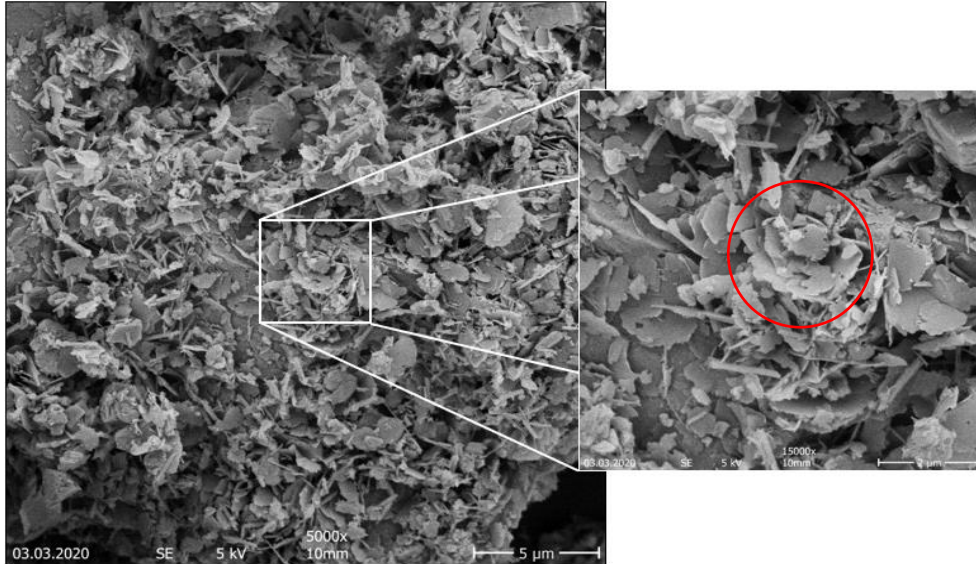


Figure 43: Mix 4, after 10 minutes hydration, AFm plates in the red circle

After 3 h mix 1 (Fig. 44) shows more hydrated phases on its surface than after 10 minutes hydration but still many empty surface areas, with no hydrates, can be observed.

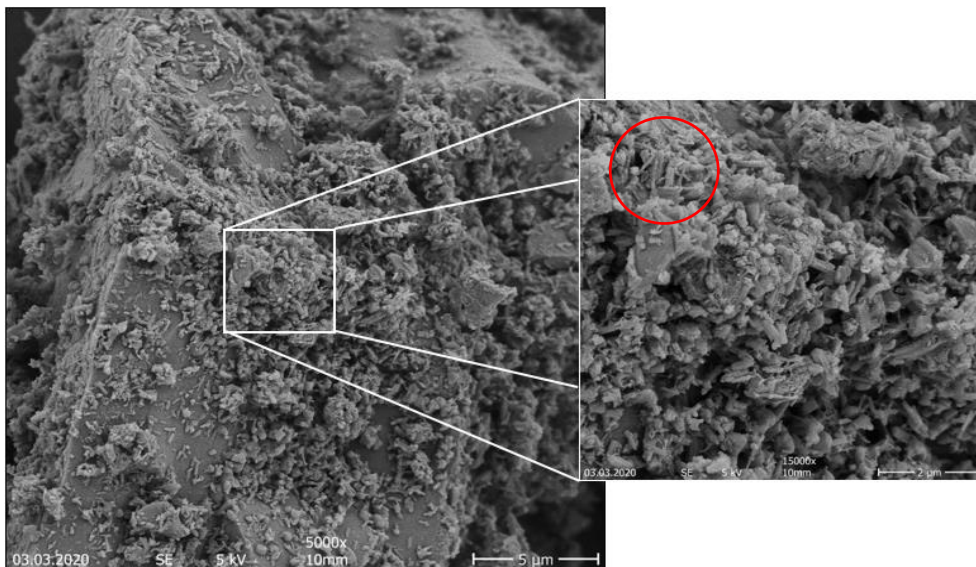


Figure 44: Mix 1, after 3 hours hydration, small ettringite needles in the red circle

Figure 45 shows mix 3, after 3 h hydration. In comparison with the same mix after 10 minutes hydration (Fig. 42), the ettringite needles seem bigger, many AFm plates are visible, and also small web-like structures have formed, evidencing early formation of C-S-H phases.

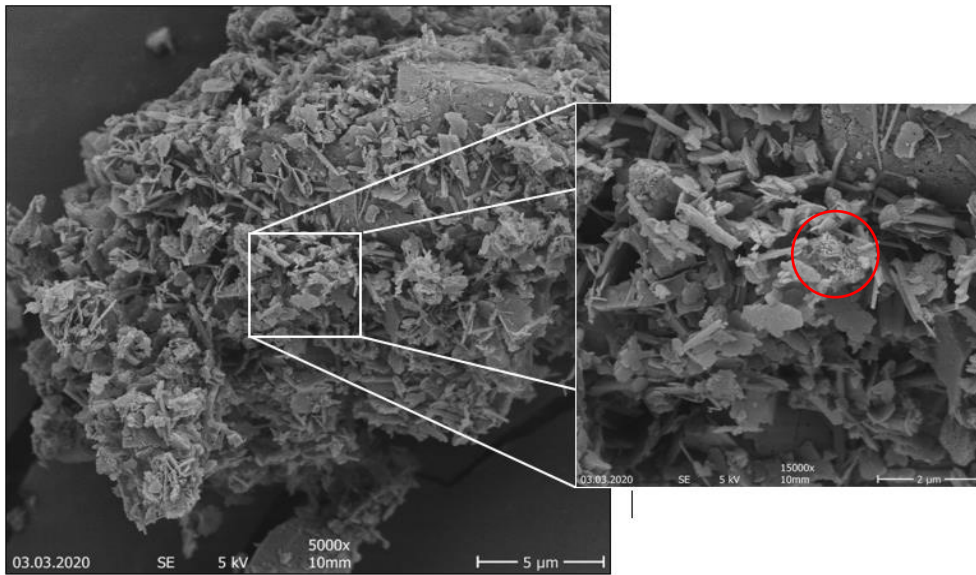


Figure 45: Mix 3, after 3 hours hydration, web-like C-S-H phases in the red circle

Similarly, mix 4 after 3 h hydration (Fig. 46) shows more ettringite needles and newly formed C-S-H web-like structures, compared to the sample after 10 minutes. Additionally, less AFm plates are visible.

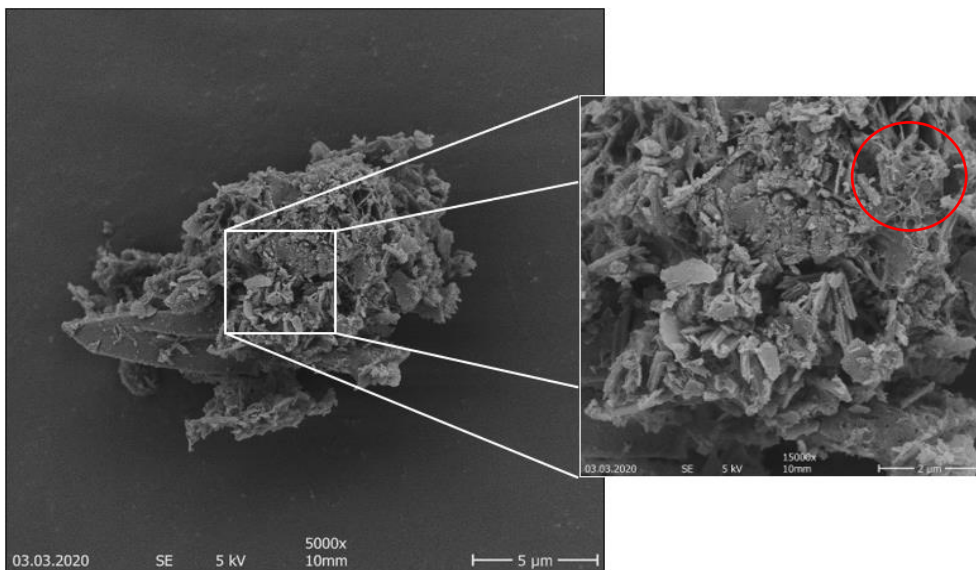


Figure 46: Mix 4, after 3 hours hydration, web-like C-S-H phases in the red circle

3.2. Real scale results

This chapter presents the results obtained from the shotcrete field tests in Wopfung. As mentioned, P-11a and P-14 mixes are similar to the laboratory mixes 3 and 4, except for the water/cement ratio (tables 7 and 8). Since the experiments in Wopfung are real shotcrete tests, mix 1 from the laboratory (100% CEM I without any kind of accelerator) is unusable

for a reference sample. Instead a mix with a commonly used spray binder is used as the reference mix P-1 (table 8).

3.2.1. Compressive early age strength development

Figure 47 shows the early-age compressive strength tests of the shotcretes. After 6 minutes P11a showed the highest compressive strength, 7 N/mm², which is up to 9 times higher than the reference mix P-1. After this time, the values remain mostly constant up to the 3rd hour when they start to increase again. Similarly, mix P14 shows constant early strength, around 4 MPa, up to the 2nd hour. Mix P-1 increases strength more steadily, reaching 1 MPa after 1 hour, and around 5 MPa after 3 hours. After 24 hours, both mixes containing CSA reach a similar value, 17 MPa, whereas the reference, mix P-1, only reaches 12 MPa. Figure 47 shows the three early age shotcrete (young shotcrete) classes J1, J2 and J3 after EN 14487-1 as well. P11a and P14 remain in J3 field at all times, making it suitable for highly unstable rock and water leakage in underground construction (Sika shotcrete manual, 2012).

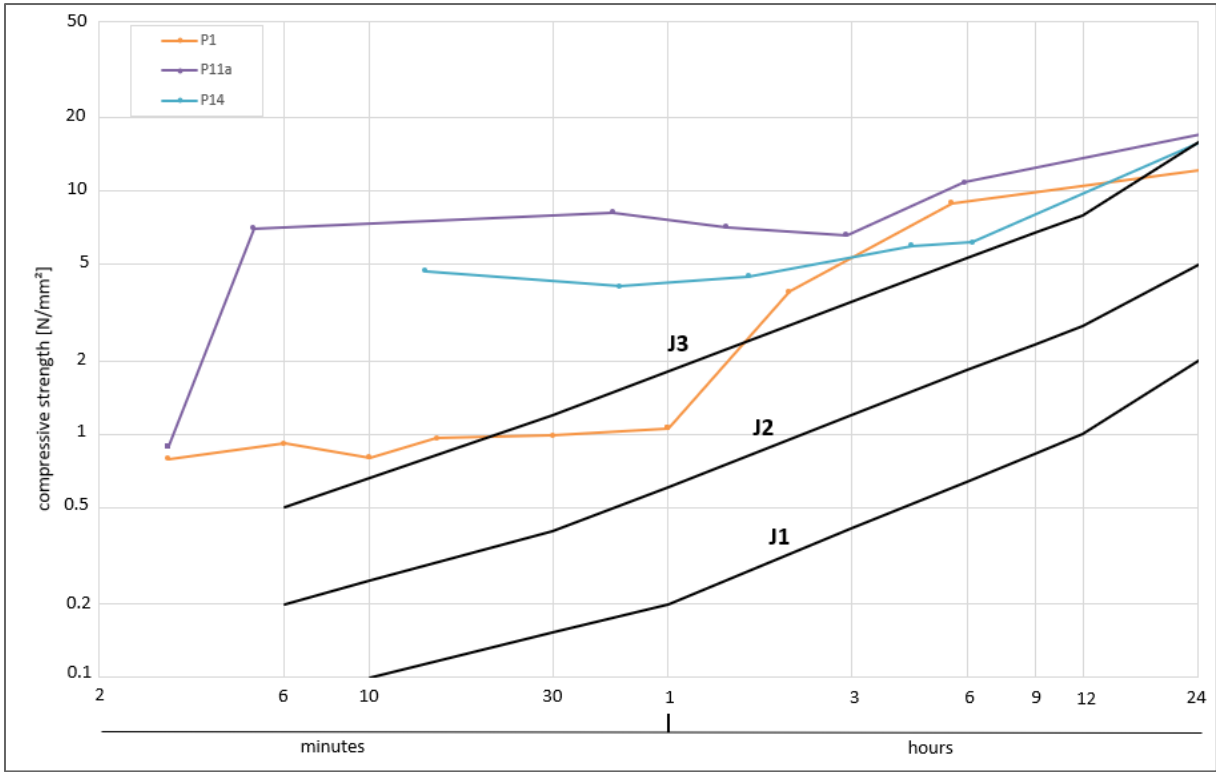


Figure 47: compressive strengths of the first 24h after application of mix P1, P11a and P14. The three early age shotcrete classes J1, J2 and J3 (EN 14487-1) plotted as well.

3.2.2. Compressive strength

Figure 48 shows the compressive strength of the 3 different mixes sprayed in Wopfung after 1, 28 and 90 days.

The results after 28 days vary between 43 and 54 N/mm². All shotcretes containing CSA cement have higher values after 1 and 28 days. However, after 90 days P-11a decreases in compressive strength up to 13%. The highest result is reached by P-14 with 60.67 N/mm². Figure 49 compares the real scale compressive strength results with the laboratory compressive strength results. After 6 hours, the real scale samples reach up to 75% higher compressive strength results.

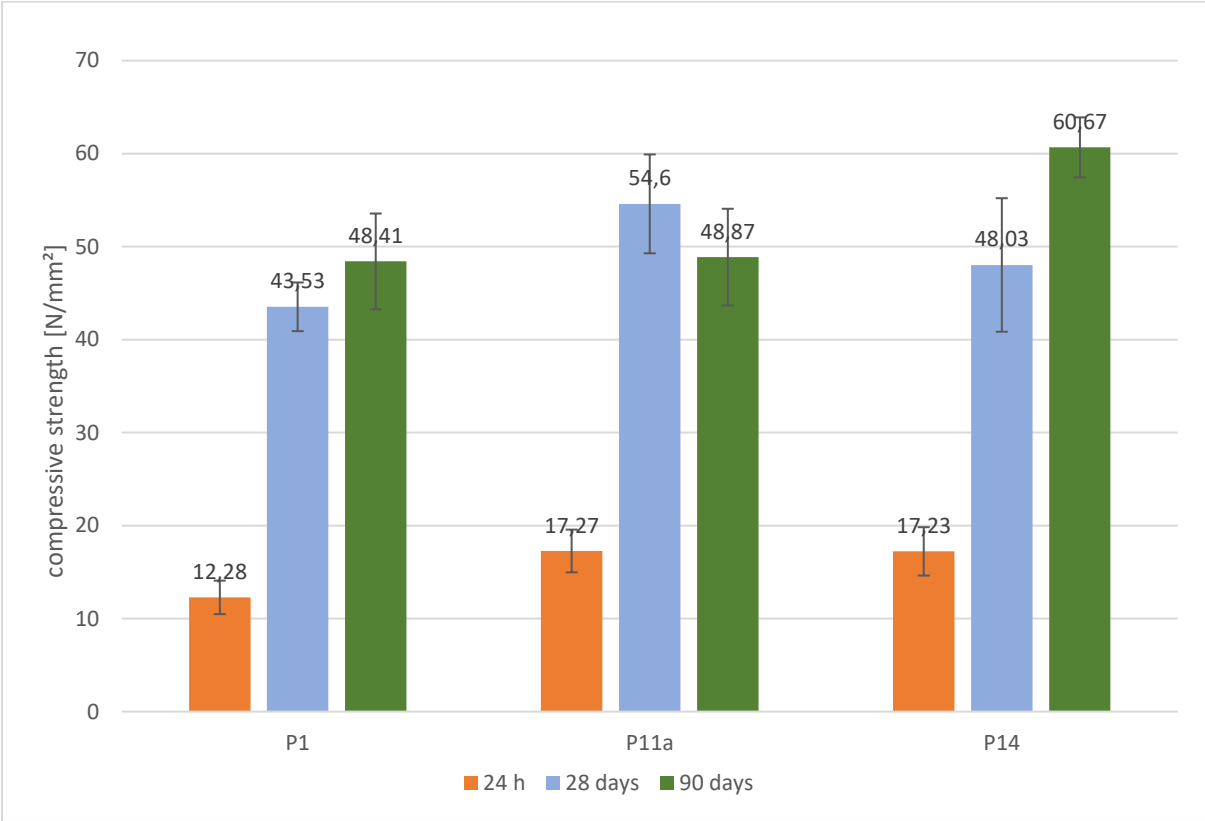


Figure 48: Compressive strengths of real scale mixes P1, P11a and P14 after 1, 28 and 90 days. (P11a = mix 3; P14 = mix 4)

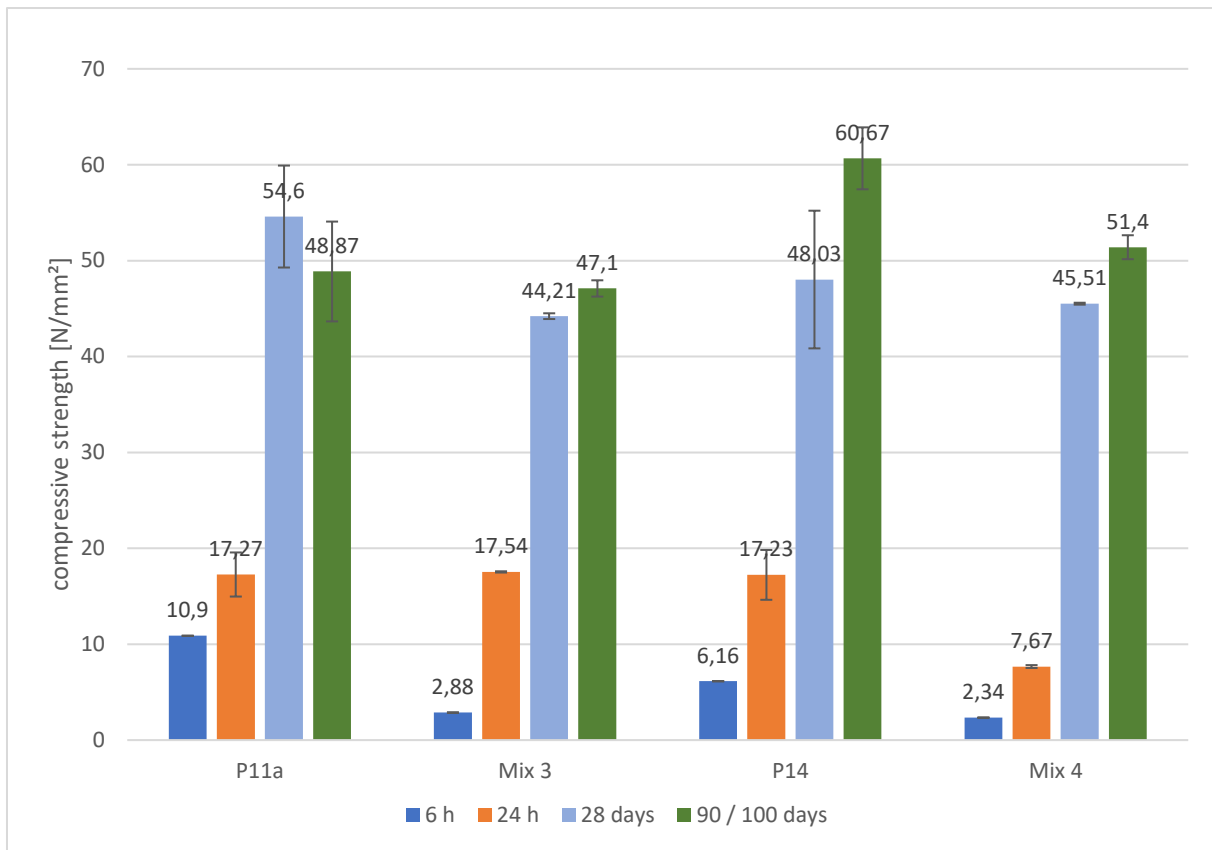


Figure 49: Real scale vs. laboratory compressive strength results after 6h, 24h, 28 days and 90 / 100 days. (P11a = mix 3; P14 = mix 4), Laboratory mixes (mix3 and 4) were measured after 100 days.

4. Discussion

Despite the vast knowledge on PC, and to a lower extent on CSA cement hydration, the combination of both systems for specific applications, like sprayed concrete, is a challenging task. Firstly, the information provided in the literature is very scarce and vague, no detailed compositions of the binders are given and in most cases the hydration reactions and phases formed were not investigated. Secondly, the ratio Al/S in the system, the source of sulfate, from calcium sulfate (as anhydrite, gypsum or hemihydrate) or from alkali sulfates, the C_3A and C_4A_3S content, etc, are all interrelated parameters which control the hydration reactions, and thus the setting and strength development. To achieve both objectives, fast setting and rapid early strength development, a fine balance between the phases responsible for both phenomena is needed: the required early (sulfo)aluminate hydrates formation should not exceed a certain threshold above which later calcium silicate hydrates formation would be inhibited/prevented.

This research work has proven that it is possible to produce suitable CSA-PC binders for dry-mix shotcrete usage. When using a CSA clinker, containing ~55% ye'elite and 30% of β and α' belite, and a CEM I cement, with ~55% alite, ~12% aluminate and various

sources of sulfate (see table 2), the optimum CSA content for achieving fast setting and high early strength was around 1%. Mixes with up to 5% CSA led to fast setting but not to high strength after 6 and 24 hours. To avoid too rapid setting, small amounts of citric acid, ~0.1% bwb, can be added to the binder, allowing for a slightly longer workability and without any detrimental consequences. The experiments of Winnefeld et al. (Winnefeld et al., 2013) show that low dosages of citric acid (~0.1%) have a very low influence on the hydration kinetics, whereas higher dosages (up to 0.5%) retard the dissolution of ye'elite, prohibiting the formation of ettringite. The research claims that the sorption and/or precipitation of the citrate ions on the cement particles surface causes the retardation (Winnefeld et al., 2013). However, in this research the visual tests of mix 3 (0.1% CA) showed a ~20 second retardation of the setting time. This means citric acid helped to reach the goal of a 60 seconds setting time without prohibiting the formation of ettringite in a large extent, which proved to be ideal for the real scale shotcrete application.

The study and evaluation of these type of systems requires both laboratory and real scale methods. In the lab, pastes and mortars were tested and analysed: XRD, isothermal calorimetry, SEM and compressive strength tests allowed for (i) the monitoring of the hydration process, (ii) the assessment of the mechanical properties and (iii) the understanding of the interrelation between both. The phases responsible for the fast setting and the high very early strength in the produced PC-CSA systems are (sulfo)aluminate hydrates, including ettringite and AFm phases, which form needles and plates, respectively, at very early stages of hydration (15 minutes). If properly designed, the silicate reaction (alite hydration: C-S-H and portlandite formation) starts to be prominent after ~3 hours and continues over the first day, being responsible for the further strength gain.

Real scale tests are needed to validate lab tests and confirm the suitability of the binders for their use in shotcrete applications. The high velocity application of the shotcrete and the nozzle man's own handling of the water/cement ratio are two of the main differences between lab accelerated mixes and real scale sprayed samples. In most cases, a much denser concrete is obtained through spraying. This leads to higher early strength values in real scale spraying tests than in lab mortar samples, up to 4 times higher after 6 hours (Fig. 49).

Another difference between lab and real scale is the storage of the samples. During the real scale tests in Wopfing, the shotcrete panels were kept for the first 24h at ambient temperature, which at certain times reached 30°C. After taken the drill cores, they were

stored at lab conditions (20°C) under water. Even though the real scale had a lower w/b ratio, the final strength was up to ~15% higher compared to the lab tests (Fig.49).

As a result, of the higher compaction and the higher outside temperatures, the overall reaction speed and the interior temperatures of the shotcrete panels from the real scale were most likely higher compared to the lab samples. This could have led to a different phase assemblage and/or some water might have evaporated during the early hydration and hardening processes. Overall leading to observed higher early strength development (e.g. 75% at 6 hours for P11a) and similar (P11a/90 days) or even higher final strength (P14/90days) . It cannot be completely ruled out that the under water storage after the real scale tests have “re-activated” certain hydration reactions resulting in an increase of volume through forming new hydration products. For instance, a small contribution of delayed ettringite formation (DEF) due to high temperatures (70-80°) during the early hydration process (Larosche, 2009) might have led to microcracks in the existing shotcrete from the real scale tests leading to the observed strength development lab vs. real scale. However, further investigation such as micro structural and mineralogical would be needed to either confirm or reject this hypothesis on the micro crack formation in the real scale samples.

The results obtained from the study have proven that CSA can be added as an accelerator to PC binders to be used for dry-mix shotcrete applications. Similar to the results of Paglia et al., (Paglia et al., 2001) small amounts of CSA accelerated the hydration process. One of the main differences in the experimental approach was that he considered CSA as a component of the accelerator, the rest being aluminium sulfate (AS). However, he also performed experiments with CSA to compare the effect of the accelerator constituents. The addition of 1.6% CSA led to a slight reduction of the setting time of PC mortars (with initial setting time of 6-7 hours), to 4-5 hours, compared to the strong reduction achieved with 6% of CSA-AS accelerator, 15-40 minutes. According to Paglia, less ettringite formed in the CSA mix than in the CSA-SA one. Similarly, the acceleration of C₃A and C₃S hydration was much more pronounced in the CSA-SA than in the CSA mix. The visual tests during this present research showed that mixes with more than 5% CSA have slower setting times compared to mix 3 (1% CSA). The compressive strength of the two mortar compositions (w/c 0.56 without plasticizer; w/c 0.46 with plasticizer) made by Paglia after 1 and 28 days are plotted in Fig. 50 (Paglia, 2000). The high w/c ratio samples show slightly lower results compared to mix 3; the low w/c ratio samples, however, showed slightly higher values than mix 3. Because the composition of the concrete is not the same, the effect of the CSA cannot

be analysed independently. Additionally, the CSA cement used by Paglia did not contain any belite; instead it was comprised of >30% of very low reactive phases.

Weifeng et al., (2018) made similar experiments investigating the behaviour of PC with increasing amounts of CSA. One of his blends consisted of 1% CSA and 99% PC and it showed the highest value of the calorimetric heat flux at 7 mW/g. That is about 87% less than the heat flux of mix 3 (present experiments) during the pre-induction period (56 mW/g). For this sample, Weifengs XRD analysis only detected small amounts of ettringite in the first 30 minutes. The setting time decreased with increasing CSA content, up to 20% CSA, when the shortest setting time was achieved. The 1% CSA samples showed initial and final setting times of 100 and 125 minutes, respectively, which were 20 and 60 minutes shorter than in the case of the sample without CSA. The CSA cement used by Weifeng et al. consisted of 15% anhydrite, which is comparable with the Vicat Alpenat R² CSA cement. During present research, samples with Vicat Alpenat R² failed to harden fast enough for shotcrete requirements. However, after 1 and 28 days Weifengs results show similar compressive strengths than Mix 3 (Fig. 50).

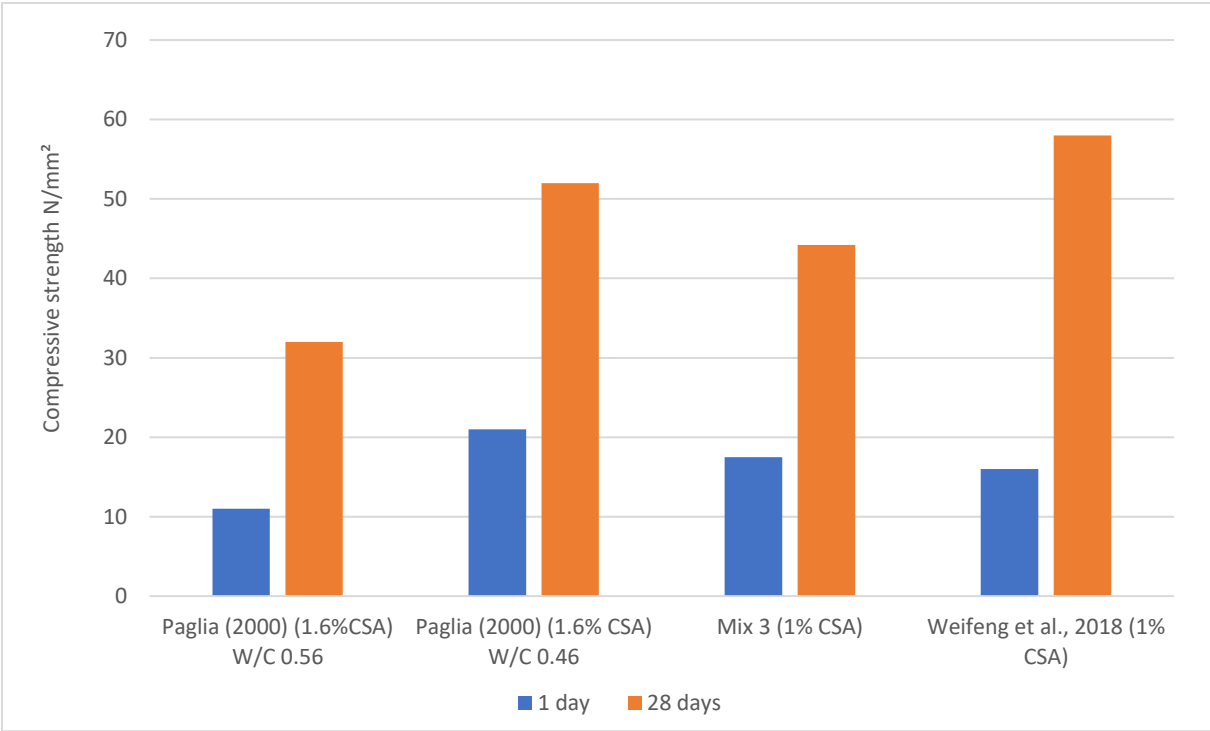


Figure 50: Comparison of laboratory compressive strength results of Paglia (2000) (1.6% CSA) without plasticizer (W/C 0.56), Paglia (2000) (1.6% CSA) with plasticizer (W/C 0.46) and Weifeng et al., 2018 (1% CSA) after 1 and 28 days with Mix 3

Considering the higher price of commercial accelerators, CSA/PC mixes have economic advantages, and they do not require the use of special binders. Additionally, the higher early strength values obtained in real scale sprayed samples compared to lab prisms indicates that

higher than 20% replacement of PC are possible without compromising the early strength. Even the use of sulfate resistant cements, with very low C_3A , may be possible if the ratio CSA/PC is properly adjusted. In any case, the durability of the newly developed mixes would need to be assessed. Further work should also include the possible use of CSA for wet-mix shotcrete. This latter is even more challenging than the present work because of the workability requirements. The concrete should remain workable until the accelerator is added; however, retarding a CSA-PC mix implies in many cases that no further acceleration is possible.

5. Conclusions

Within this work the influence of CSA mixed with PC was investigated and a suitable mix for dry-mix shotcrete was created. The main conclusions are:

- Small amounts of CSA cement work like an accelerator in the PC/CSA system. Ye'elemite from the CSA cement supports the ettringite formation during the first minutes of hydration, resulting in good early age strength results. Mixes with 1% CSA could keep the balance between the early (sulfo)aluminate hydrate formation and the later calcium silicate hydrate formation to gain maximum strength.
- Citric acid works like a retarder in the PC/CSA systems and 0.1% slowed down the reaction for about 20 seconds, which prevented too fast setting and made mixes with 0.8-1% CSA suitable for dry-mix shotcrete applications.
- The high outside temperature had an impact on the hydration mechanisms between 24 h and 90 days, especially in the mix without GGBS, resulting in a loss of compressive strength. Evaporation of pore water, possibly together with the lower cement/water ratio used in the real scale tests, interfered with the hydration process of the cement. Therefore, a better storage concept or watering the fresh shotcrete for the first hours would probably increase the compressive strength after 28 and 90 days.
- Using GGBS in one of the PC/CSA mixes contributed to a strength gain between 28 and 90 days both in the lab and in the real scale experiments, reaching higher values

than the mixes without GGBS. This is attributed to the latent hydraulic reaction of the GGBS supporting the C-S-H formation, which is the strength giving phase of the cement matrix.

- The real scale tests showed that mixes with CSA achieved much higher compressive strengths in the first 24h after application than the laboratory tests because of the compaction of the concrete due to the spraying method. Because of these results, the assumption can be made that even more than 20% of the mix can be replaced with GGBS without compromising the early strength.

References

Ambroise J., Pera J., 2008. “*Use of calcium sulfoaluminate cement to improve strength of mortars at low temperature*”, Concrete Repair, Rehabilitation and Retrofitting II: 2nd International Conference on Concrete Repair, ISBN- 978-0-415-46850-3

Austrian Building Technology Association (ÖBV), 2013. “*Guideline: Sprayed Concrete.*”

Bescher E., Ocampo N., Ballou M., 2013. “*The use of calcium sulfoaluminate rapid setting cement*”, Tunnel Business Magazine, October 2013

Cengiz, L Turanli, 2004. “*Comparative evaluation of steel mesh, steel fibre and high-performance polypropylene fibre reinforced shotcrete in panel test*”, Cement and Concrete Research, Volume 34, Issue 8, ISSN 0008-8846

Galan I., Briendl L., Hoedl M., Steindl F., Juhart J., Mittermayr F., 2019. “*Early hydration of dry-mix sprayed concrete*”, 1st International Conference on Innovation in Low-Carbon Cement and Concrete Technology, June 2019

Gartner E., Walenta G., Morin V., Termkhajornkit P., Baco I., Casabonne J., 2011. “*Hydration of a Belite-CalciumSulfoaluminateFerrite cement: AetherTM*” 13th International Congress on the Chemistry of Cement

Glasser F.P., Zhang J.L., 2001. “*High-Performance Cement Matrices Based on Calcium Sulfoaluminate–Belite Compositions*”, Cement and Concrete Research, Volume 31, Issue 12, ISSN 1881-1886

Habert G., 2014. “*Assessing the environmental impact of conventional and ‘green’ cement production*”, Eco-efficient Construction and Building Materials, Woodhead Publishing, 2014, Pages 199-238, ISBN 9780857097675

Höfler J., Schlumpf J., Jahn M., 2012. “*Sika Sprayed Concrete Handbook*”, Sika AG, Edition 4, August 2012

- Juenger M., Winnefeld F., Provis J., Ideker J., 2011. “*Advances in alternative cementitious binders*”, Cement and Concrete Research, Volume 41, ISSN 1232–1243
- Klein A. 1963, “*Calciumaluminosulfate and expansive cements containing same*”, US Patent No. 3, 155, 526
- Larosche C.J., 2009. “*Types and causes of cracking in concrete structures.*”, Woodhead Publishing Series in Civil and Structural Engineering, Pages: 57-83, ISBN 9781845694081
- Lothenbach B., Scrivener K., Hooton R.D., 2011. “*Supplementary cementitious materials*”, Cement and Concrete Research, Volume 41, Issue 12, ISSN 0008-8846
- Mehta P.K., 1987. “*Natural pozzolans: Supplementary cementing materials for concrete*”, CANMET Special Publication 86:1-33
- Meller N., Hall, Jupe A., Colston S. L., Jacques S. D. M., Barnes P., Phipps J., 2004. “*The paste hydration of brownmillerite with and without gypsum: A time resolved synchrotron diffraction study at 30, 70, 100 and 150 °C*”, Journal of Materials Chemistry, Issue 3
- Myrdal R., 2007. “*Accelerating Admixtures for Concrete. State of the Art*”, SINTEF Report, A07025
- Nkinamubanzi P.C., Mantellato S., Flatt R.J., 2016. “*Science and technology of concrete admixtures*”, Woodhead Publishing, Pages: 353-357
- Oberlink A., Robl T., Jewekk R., Duvallet T., Mills P., Jones M.R., 2016. “*Rapidly deployable shotcrete system for the structural stabilization of schock damaged structures*”, 9th International Concrete Conference 2016
- Paglia C., 2000. “*The influence of calcium sulfoaluminate as accelerating component within cementitious systems*”, ETH Zurich, Switzerland
- Paglia C., Wombacher F., Böhni H., 2001. “*The influence of alkali-free and alkaline shotcrete accelerators within cement systems*”, Cement and Concrete Research, Volume 31, Issue 6, ISSN 0008-8846
- Reny S., Clements W., 2013. “*Reaching 20 MPa (2900 psi) in 2 Hours is Possible*”, Shotcrete Corner, Fall 2013
- Salvador R.P., Cavalaro S.H.P., Figueiredo A.D., Perez J., 2016. “*Early age hydration of cement pastes with alkaline and alkali-free accelerators for sprayed concrete*”, Construction and Building Materials 111: 386–398
- Sharp J.H., Lawrence C.D., Yang R., 1999. “*Calcium sulfoaluminate cements—low-energy cements, special cements or what?*”, Advances in Cement Research, No. 1, Pages 3-13
- Sjölander A., Gasch T., Ansell A., Malm R., 2016. “*Shrinkage cracking of thin irregular shotcrete shells using multiphysics models*”, 9th International Conference on Fracture Mechanics of Concrete and Concrete Structures, DOI: 10.21012/FC9.140
- Sprayed Concrete Association, 2016. “*Introduction to Sprayed Concrete*”, August 2016

- Srivastava V., Yadav R., 2019. “*Data Processing Handbook for Complex Biological Data Sources*”, New and Future Developments in Microbial Biotechnology and Bioengineering, Elsevier, ISBN-13: 9780444642233
- Tadolini A.C., Mills P.S., Burkhard D.R., 2017 “*Tekcrete Fast: Fiber-reinforced, rapid-setting sprayed concrete for rib and surface control*”, International Journal of Mining Science and Technology, Issue 28, Chapter: 29-34.
- Teichert P., 2002. “*Carl Akeley – A Tribute to the Founder of Shotcrete*”, Shotcrete Magazine, Summer 2002
- Thornton T., Rex A., 1993. “*Modern Physics for Scientists and Engineers*”, Saunders College Publishing
- Tikkanen A., Lotha G., 2019. “*Shotcrete*”. Encyclopaedia Britannica (<https://www.britannica.com/technology/shotcrete>, page visited: 01.14.2020)
- Wang, J., Baco I., Morin V., Walenta G., Damidot D., Gartner E., 2010. “*Hydration mechanism of cements based on low-CO₂ clinkers containing belite, ye'elimite and calcium alumino-ferrite*”, The 7th International Symposium on Cement and Concrete, ISCC2010
- Weifeng L., Jin Y., Suhua M., Yueyang H., Dashun G., Xiaodong S., 2018. “*The Properties and Hydration of Portland Cement containing Calcium Sulfoaluminate Cement*”, Ceramics-Silikaty 62 (4), Pages 364-373
- Winnefeld F., Klemm S., 2013. “*Influence of citric acid on the hydration kinetics of calcium sulfoaluminate cement*” 1st International Conference on Sulphoaluminate Cement: Materials and Engineering Technology, Page 288-308, October 2013
- Yu, H., Wu L., Liu W., Pourrahimian Y., 2017. “*Developing shrinkage-compensating shotcrete mixtures from calcium sulfoaluminate, portland cement, and calcium sulfate*”, CIM 2017 Convention
- Yu H., Wu L., Liu W., Pourrahimian Y., 2018. „*Effects of fibers on expansive shotcrete mixtures consisting of calcium sulfoaluminate cement, ordinary Portland cement, and calcium sulfate*”, Journal of Rock Mechanics and Geotechnical Engineering, Volume 10, Issue 2, Pages 212-221
- Zhang J.L., Glasser F.P., 1999. “*New concretes based on calcium sulfoaluminate cement*”, Proceedings of the International Conference on Modern Concrete Materials: Binders, Additions and Admixtures, Thomas Telford, Pages 261–274

Appendix

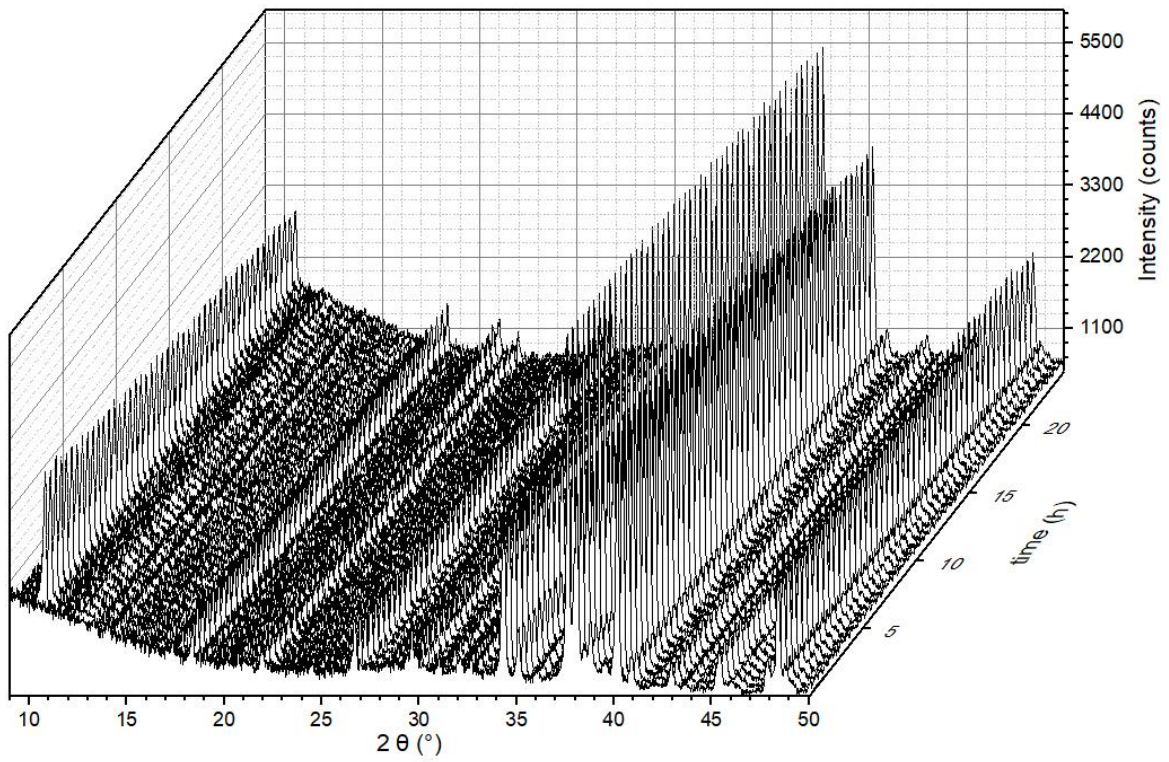


Figure 51: 24h In-situ-XRD measurement of mix 1

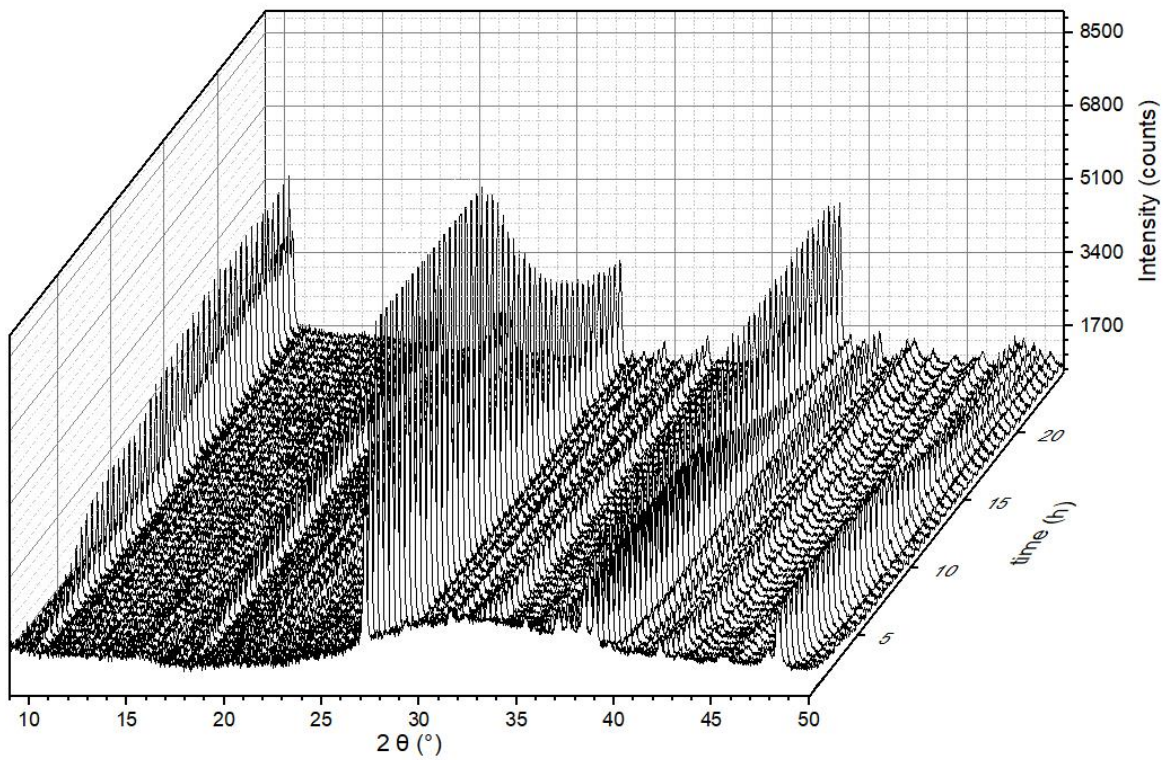


Figure 52: 24h In-situ-XRD measurement of mix 2

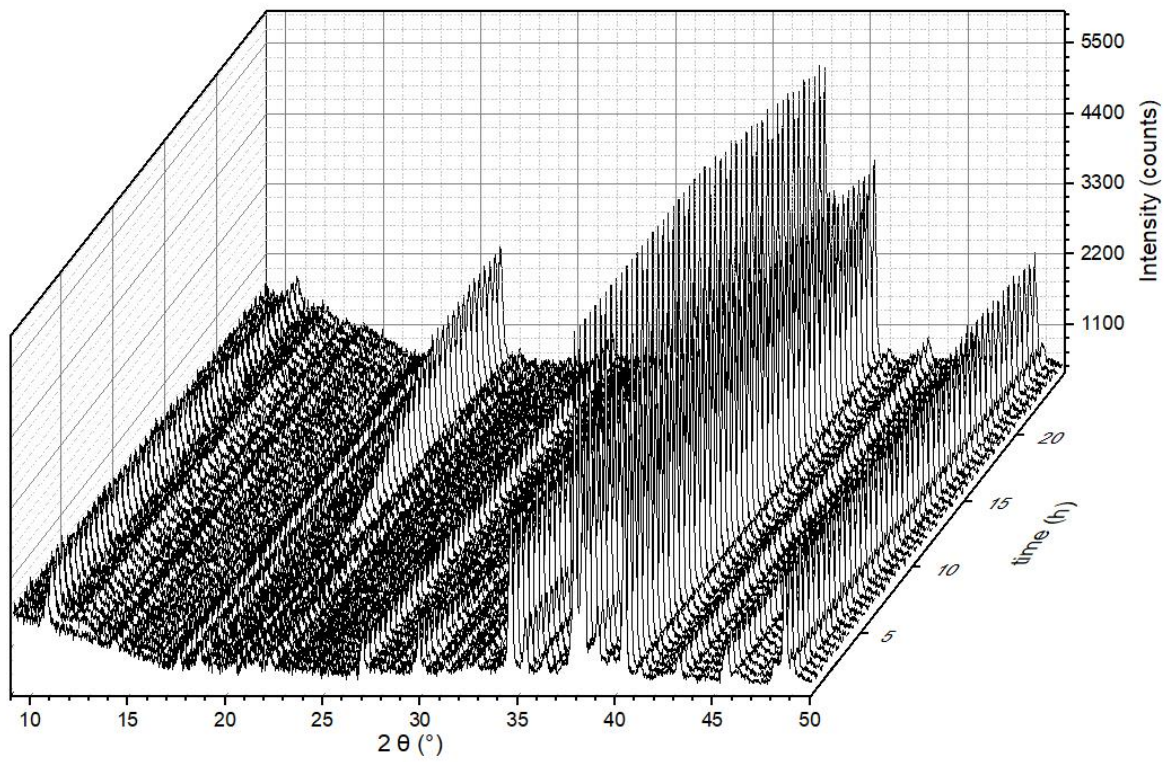


Figure 53: 24h Insitu-XRD measurement of mix 3

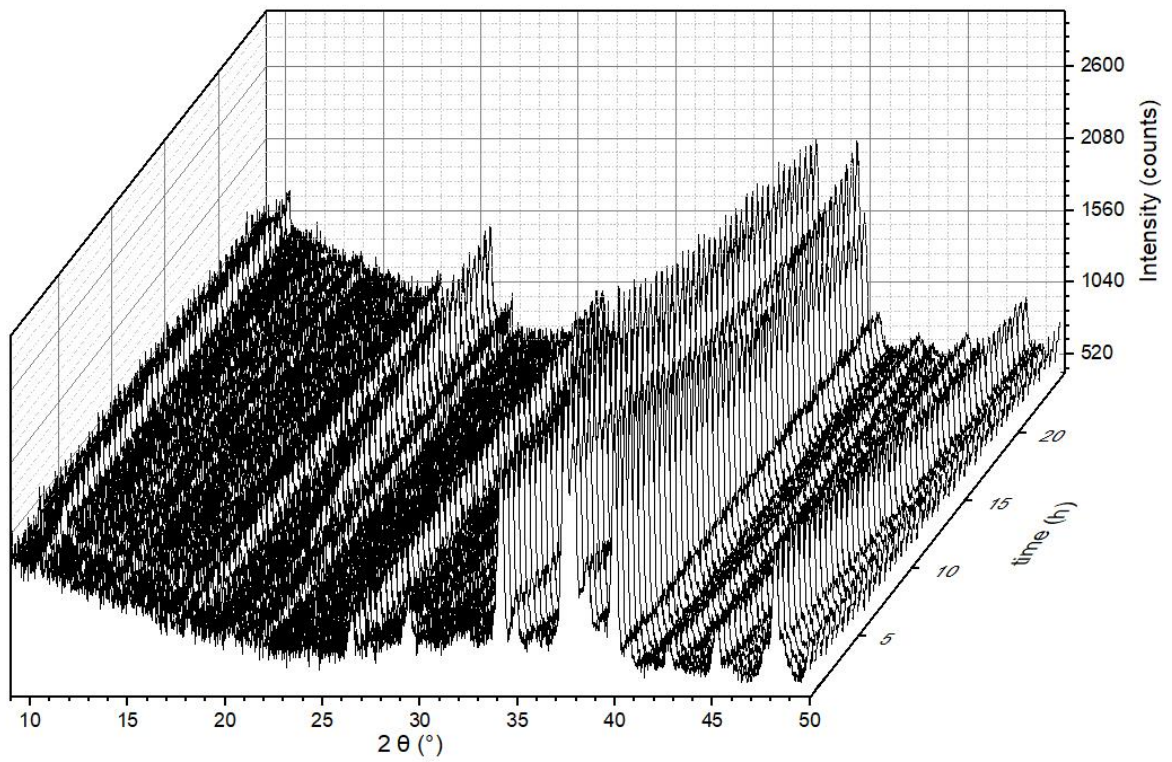


Figure 54: 24h Insitu-XRD measurement of mix 4

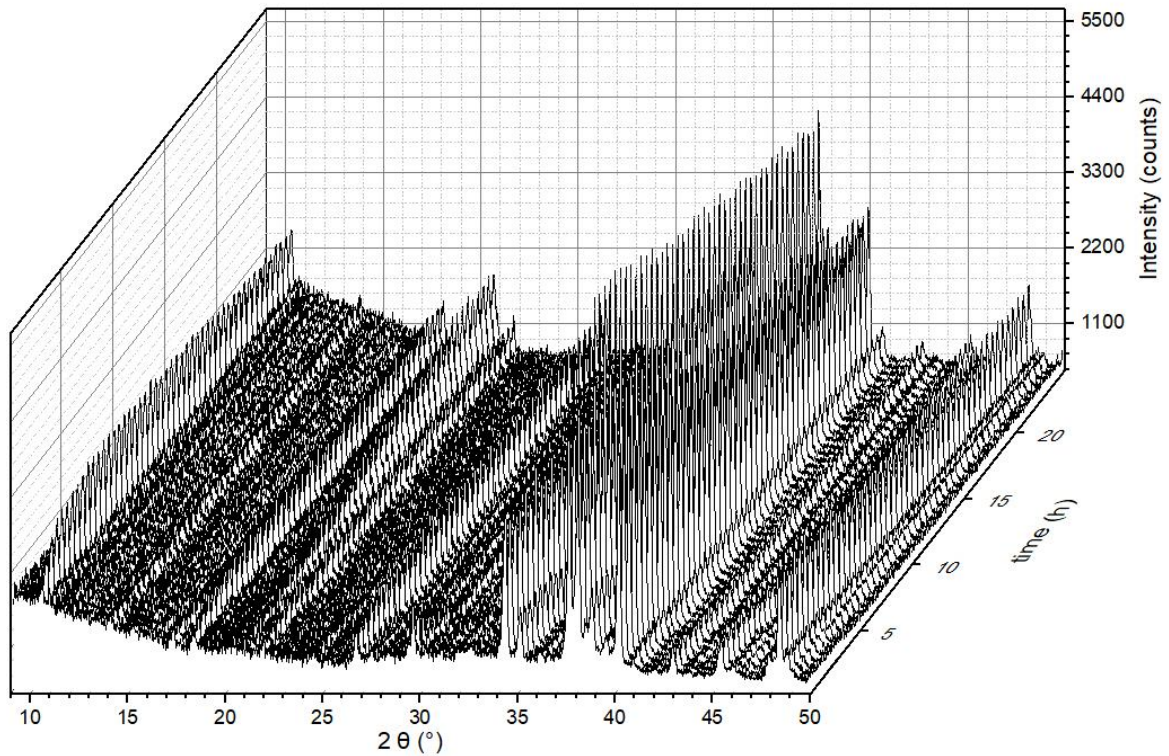


Figure 55: 24h Insitu-XRD measurement of mix 5

List of tables

Table 1: Typical mixing ratios of wet-mix and dry-mix shotcretes.....	7
Table 2: Mineralogical composition of CEM I, SR0 and spray binder (- = below detection limit).....	12
Table 3: Chemical composition of CEM I, SR0, spray-binder and GGBS (- = below detection limit).....	12
Table 4: Mineralogical composition of Alpenat CK and Alpenat R ² (- = below detection limit)	13
Table 5: Chemical composition of Alpenat CK and Alpenat R ²	13
Table 6: Density and particle size characteristics of the powdery materials used	14
Table 7: Binder composition of the 22 tested mixes.....	16
Table 8: Composition of the 3 different mixes tested and sprayed in Wopfing.	16
Table 9: List of the different methods used to analyse the lab mixes. Positive visual tests are highlighted green.	27

List of figures

Figure 1: Shotcrete-stabilized cliff wall (Tikkanen et al., 2019)	1
Figure 2: Primary tunnel linings (Sprayed Concrete Association, 2016)	2
Figure 3: Simplified display of wet-mix-process (Sprayed Concrete Association, 2016)	2
Figure 4: Simplified display of dry-mix-process (Sprayed Concrete Association, 2016)	3
Figure 5: Grain size distribution of dolomite Eberstein and sand Bad Fischau according to ÖNORM B 3131.....	15
Figure 6: I-CAL 4000 HPC at TU Graz Inffeldgasse	17
Figure 7: Heat flow curve of reference Mix 1.....	18
Figure 8: ToniPRAX compressive strength testing machine at TU Graz Inffeldgasse.....	19
Figure 9: ToniPRAX flexural strength testing machine at TU Graz Inffeldgasse.....	19
Figure 10: Prism-steel-case placed on the shaker before the mortar was poured in.....	20
Figure 11: Bragg's Law (Thornton et al., 1993)	21
Figure 12: Sample changer and measurement device inside the Panalytical X'Pert Pro.....	21
Figure 13: X-Ray diffractometer Panalytical X'Pert Pro at TU Graz Rechbauerstraße	21
Figure 14: Kapton film on a sample used for a 24h In-situ measurement.....	22
Figure 15: SEM Zeiss DSM 982 GEMINI	22
Figure 16: a: gold/paladium layer on the samples after coating. b: vacuum chamber of the coating device.	23
Figure 17: CEM I reference mix on the cellulose filter after the addition of isopropanol. Glass container underneath is under vacuum.....	23
Figure 18: a: Mixing device in one of the containers in Wopfing. b: Wooden boxes, where the shotcrete was sprayed and red nozzle of the spraying device.....	24
Figure 19: Needle Penetration Test carried out in Wopfing	25
Figure 20: Calibration curve (ÖNORM EN 14488-2).....	25
Figure 21: Stud driving test carried out in Wopfing	26
Figure 22: calibration curve of the stud driving method (ÖNORM EN 14488-2)	26
Figure 23: Drill machine used in Wopfing	27
Figure 24: Heat flux of mixes 1(100%CEMI), 2(100%CK), 3(1%CK-0.1%CA) and 4(20%GGBS-1%CK-0.1%CA) after 2h of hydration.....	29
Figure 25: Heat flux of mixes 1(100%CEMI), 2(100%CK), 3(1%CK-0.1%CA) and 4(20%GGBS-1%CK-0.1%CA) after 24h of hydration.....	29
Figure 26: Cumulative heat of mixes 1(100%CEMI), 2(100%CK), 3(1%CK-0.1%CA) and 4(20%GGBS-1%CK-0.1%CA) after 24h of hydration.	30
Figure 27: Heat flux of mixes 3(1%CK-0.1%CA), 6(40%CK), 7(30%CK), 8(20%CK), 15(5%CK) after 2h of hydration.	31
Figure 28: Heat flux of mixes 3(1%CK-0.1%CA), 6(40%CK), 7(30%CK), 8(20%CK), 15(5%CK) after 24h of hydration.	31
Figure 29: Cumulative heat of mixes 3(1%CK-0.1%CA), 6(40%CK), 7(30%CK), 8(20%CK), 15(5%CK) after 24h of hydration.	32
Figure 30: Heat flux of mixes 10(50%CK), 11(10%CK), 12(10%R ²), 13(1%CK-0.5%Ca(OH) ₂) and 14(100%SR0) after 2h of hydration.	33
Figure 31: Heat flux of mixes 10(50%CK), 11(10%CK), 12(10%R ²), 13(0.1%CK-0.5%Ca(OH) ₂) and 14(100%SR0) after 24h of hydration.	33
Figure 32: Cumulative heat of mixes 10(50%CK), 11(10%CK), 12(10%R ²), 13(0.1%CK-0.5%Ca(OH) ₂) and 14(100%SR0) after 24h of hydration.	34
Figure 33: XRD- scans (every 30 minutes) from 9-30° 2 θ of mix 1 up to 24h (Et=ettringite, P=portlandite, An=anhydrite).....	35

Figure 34: XRD- scans (every 30 minutes) from 9-30° 2 θ of mix 2 up to 24h (Et=ettringite, P=portlandite, Y= ye'elemite).....	36
Figure 35: XRD- scans (every 30 minutes) from 9-30° 2 θ of mix 3 up to 24h (Et=ettringite, Ms=monosulfate, P=portlandite, An=anhydrite)	37
Figure 36: XRD- scans (every 30 minutes) from 9-30° 2 θ of mix 4 up to 24h (Et=ettringite, P=portlandite, An=anhydrite).....	38
Figure 37: XRD- scans (every 30 minutes) from 9-30° 2 θ of mix 5 up to 24h (Et=ettringite, P=portlandite, An=anhydrite).....	39
Figure 38: XRD-patterns of mix 3 and mix 4 from 7-80° 2 θ measured 14 days after hydrating the cement (Et=ettringite, Ms=monosulfate, P=portlandite, A=alite, B=belite, C=calcite, D=dolomite, Pc=periclase)	40
Figure 39: Compressive strength results of mix 3 and 4 up to 100 days	41
Figure 40: Flexural strength results of mix 3 and 4 up to 100 days	41
Figure 41: Mix 1, after 10 minutes hydration, small ettringite needles in the red circle.....	42
Figure 42: Mix 3, after 10 minutes hydration, ettringite needles in the red circle	42
Figure 43: Mix 4, after 10 minutes hydration, AFm plates in the red circle.....	43
Figure 44: Mix 1, after 3 hours hydration, small ettringite needles in the red circle	43
Figure 45: Mix 3, after 3 hours hydration, web-like C-S-H phases in the red circle	44
Figure 46: Mix 4, after 3 hours hydration, web-like C-S-H phases in the red circle.....	44
Figure 47: compressive strengths of the first 24h after application of mix P1, P11a and P14. The three early age shotcrete classes J1, J2 and J3 (EN 14487-1) plotted as well.	45
Figure 48: Compressive strengths of real scale mixes P1, P11a and P14 after 1, 28 and 90 days. (P11a = mix 3; P14 = mix 4)	46
Figure 49: Real scale vs. laboratory compressive strength results after 6h, 24h, 28 days and 90 / 100 days. (P11a = mix 3; P14 = mix 4), Laboratory mixes (mix3 and 4) were measured after 100 days.	47
Figure 50: Comparison of laboratory compressive strength results of Paglia (2000) (1.6% CSA) without plasticizer (W/C 0.56), Paglia (2000) (1.6% CSA) with plasticizer (W/C 0.46) and Weifeng et al., 2018 (1%CSA) after 1 and 28 days with Mix 3	50
Figure 51: 24h Insitu-XRD measurement of mix 1	55
Figure 52: 24h Insitu-XRD measurement of mix 2	55
Figure 53: 24h Insitu-XRD measurement of mix 3	56
Figure 54: 24h Insitu-XRD measurement of mix 4	56
Figure 55: 24h Insitu-XRD measurement of mix 5	57